

## MID-INFRARED IMAGING OF STAR-FORMING REGIONS CONTAINING METHANOL MASERS

JAMES M. DE BUIZER, ROBERT K. PIÑA, AND CHARLES M. TELESCO

Department of Astronomy, University of Florida, Gainesville, FL 32601

Received 1999 December 6; accepted 2000 May 10

### ABSTRACT

We present a mid-infrared imaging survey of 21 sites of massive star formation associated with methanol masers. Images were obtained from the Cerro Tololo Inter-American Observatory 4 m Blanco telescope using the University of Florida imager/spectrometer OSCIR. Of the 10 sites where the methanol masers are distributed in a linear fashion, we find three sources that are elongated at the same position angle as their linear methanol maser distributions. It is believed that these elongated mid-infrared objects are indeed circumstellar disks. It was found that the masers may arise inside the mid-infrared emitting regions of these young stellar objects, indicating that the methanol masers may be pumped by mid-infrared photons. Many mid-infrared sources in our survey have no detectable radio continuum emission, and we advance the hypothesis that these sources are lower mass, nonionizing stars.

*Subject headings:* circumstellar matter — infrared: stars — masers — stars: formation — stars: pre-main-sequence

### 1. INTRODUCTION

Radio emission from molecular species such as hydroxyl (OH) and water (H<sub>2</sub>O) have been observed for several decades and is a well-known indicator of recent massive star formation. These masers occur in spatially localized regions or “spots” and serve as powerful probes of the small-scale structure, dynamics, and physical conditions of the environments near forming stars. The associated infant stars are known as “young stellar objects” (YSOs), and in the vicinity of some YSOs are ultracompact regions of ionized gas, or “UC H II regions”. High emission measures ( $> 10^7$  pc cm<sup>6</sup>) and high electron densities ( $> 10^4$  cm<sup>3</sup>) are characteristic of UC H II regions. Since UC H II regions can be observed via their free-free continuum emission at radio wavelengths, several radio surveys have been performed to try to understand the spatial relationship of the UC H II regions and their associated masers (Caswell 1996, 1997; Hofner & Churchwell 1996).

Maser emission from the methanol (CH<sub>3</sub>OH) molecule has in the recent decade become the subject of intense investigation. There are two classes of methanol maser, distinguished by their locations with respect to YSOs and by the transitions in which they mase. Class II masers are coincident with UC H II regions associated with YSOs, whereas Class I masers are offset by typically a parsec. Class I sources show enhanced absorption at 12 GHz, whereas Class II masers in this transition. Originally designated Class A and B, the classes were switched by Menten (1991a) to avoid confusion with the A and E species of methanol. Both Class I and Class II maser sites show masing in both A and E species.

This paper focuses on two strong Class II masing transitions of methanol that most closely delineate the sites of formation of high mass stars. These are the 12.2 GHz  $2_0 \rightarrow 3_{-1}$  E transition, which was first discovered by Batrla et al. (1987), and the 6.7 GHz  $5_1 \rightarrow 6_0$  A<sup>+</sup> transition, which was first detected by Menten (1991b).

The first high spatial resolution images of methanol at 12.2 GHz were obtained by Norris et al. (1988). It was found that, like OH and H<sub>2</sub>O masers, methanol masers generally exist as groups of maser spots. Radio observations by Norris et al. (1993) have shown that 6.7 and 12.2 GHz meth-

anol maser spots are often distributed in linear structures, with projected dimensions typically spanning several thousand AU. Furthermore, these maser spots in some cases appear to exhibit Keplerian motions (as determined by the frequency shift of the maser line) indicative of orbital motion. It has thus been argued that these linear methanol maser spots occur in, and directly delineate, rotating circumstellar disks. A direct consequence of this hypothesis is that the methanol masers should be exactly coincident with the embedded young stars they are orbiting. A survey of 97 methanol maser sites by Walsh et al. (1998), has shown that well-defined linear maser distributions occur in 9% of their survey, and another 28% of the sites have some semblance of linearity. They conclude that the proclivity for methanol masers to exist in linear distributions is not ubiquitous, but it does occur a statistically significant number of times in their survey.

The interpretation of the linear methanol maser distribution found by Norris et al. (1993) was hampered by lack of complementary information about the sites at other wavelengths. Only in recent years have radio continuum images of UC H II regions associated with methanol masers been obtained (e.g., Walsh et al. 1998; Phillips et al. 1998). Optical imaging is not useful because these massive stars are presumably heavily embedded in their birth clouds and are totally obscured visually. However, because infrared radiation is much less affected by extinction than visible radiation, infrared images can probe through the cool obscuring dust. Furthermore, mid-infrared images (5–25  $\mu$ m) can trace the radiation from the  $T \sim 200$  K dust close to the stellar sources associated with the methanol masers, and could even detect circumstellar disks around these stars if they exist. The main motivation of this mid-infrared survey was to locate the stellar sources associated with the methanol maser emission and to determine what stellar process or processes methanol maser emission is tracing.

This paper presents a mid-infrared imaging survey of 21 methanol maser sites observed in the radio methanol survey by Norris et al. (1993). Section 2 contains a discussion of the observations. Section 3 presents the data reduction methods and results. Section 4 contains a review of what is known about the individual sources and presents our mid-

infrared images. Section 5 is our discussion section, and conclusions are presented in § 6.

## 2. OBSERVATIONS

Observations were carried out at Cerro Tololo Inter-American Observatory (CTIO) on the Victor M. Blanco 4 meter telescope using the University of Florida mid-infrared imager/spectrometer OSCIR. This instrument employs a Rockwell  $128 \times 128$  pixel Si:As blocked impurity band (BIB) detector array, which is optimized for wavelength coverage between 8 and  $25 \mu\text{m}$ . The field of view of the array at CTIO is  $23'' \times 23''$ , with a scale of  $0''.183 \text{ pixel}^{-1}$ . Sky and telescope emission were removed using the standard chop-nod technique.

The methanol maser sites were observed on the evenings of 1998 July 2 and 3, under very clear skies with low relative humidity ( $<20\%$ ) and at low air masses ( $<1.2$ ). Images were taken using OSCIR's broadband  $N$  ( $\lambda_o = 10.46 \mu\text{m}$ ,  $\Delta\lambda = 5.1 \mu\text{m}$ ) and IHW18 (International Halley Watch,  $\lambda_o = 18.06 \mu\text{m}$ ,  $\Delta\lambda = 3.0 \mu\text{m}$ ) filters with 2 minute chopped integration (i.e., on source plus off source) times, except for the G339.88–1.26 images, which were taken with 4 minute chopped integration. The primary standard star for these observations was  $\eta$  Sgr, for which the flux densities were taken to be 188 Jy at  $N$  and 66 Jy at IHW18. However,  $\eta$  Sgr is a known variable star, so we observed a secondary standard  $\beta$  Gru, whose calibration correction agreed with that of  $\eta$  Sgr to a few percent.

Table 1 lists the targets in this survey. The coordinates listed are the reference maser spot positions given by Norris et al. (1993), which were obtained with a connected element interferometer and have absolute positional accuracies better than  $0''.5$ . The mid-infrared absolute astrometry was obtained by offsetting the telescope to the maser reference coordinates from nearby reference stars (typically about  $10'$  away) whose coordinates were obtained from the Positions and Proper Motions South Catalogue (PPM/South). The

absolute pointing accuracy of the telescope was estimated to be about  $2''.5$ , determined by repeatedly offsetting between reference stars. We therefore conclude that the relative accuracy of the astrometry between the maser reference features and our pointing is also  $2''.5$ . One further note of caution is that there were also occasionally large non-reproducible offsets from  $3''$  to  $6''$  when the telescope was slewed from one reference star to another. This may account for some of the larger offsets observed between the maser reference positions and mid-infrared sources.

Point-spread function (PSF) stars were imaged near the positions of most of the targets. Error in the PSF size was taken to be the standard deviation of the size of the PSF stars imaged throughout the night. A target object was considered to be resolved if the measured full width at half-maximum (FWHM) was greater than three standard deviations from its closest PSF FWHM. Marginally resolved objects are between 2 and 3 standard deviations of the PSF FWHM.

## 3. DATA REDUCTION AND RESULTS

Of the 21 sites we observed in the mid-infrared, we had seven nondetections (Table 1). Table 2 lists the sites where detections were made and the corresponding flux densities. Many sites contained multiple sources which are labeled 1, 2, 3, etc.<sup>1</sup> so they can be addressed individually (see Figs. 1–13). The sites where no detections were found are listed with a  $3\sigma$  upper limit for a point-source flux density.

Because of the large bandwidth of the filters, the observed fluxes must be color corrected to account for the intrinsic source spectrum, the filter transmission, and the atmospheric transmission. For the calibration star, the spectrum was assumed to be a blackbody at the effective stellar temperature. Color corrected monochromatic flux densities, dust color temperatures, and optical depth values were obtained in a self-consistent manner by numerically integrating the product of the Planck function, emissivity function (given by  $1 - e^{-\tau_\lambda}$ , where  $\tau_\lambda$  is given by the Mathis 1990 extinction law), filter transmission, solid angle subtended by the source, and model atmospheric transmission through the filter bandpass. For resolved sources, the source sizes were taken to be the  $N$ -band FWHMs subtracted in quadrature from the PSF FWHM (§ 1 of Table 2). For unresolved sources, calculations were made using the blackbody limiting sizes and the resolution limiting sizes (taken to be  $0''.55$  at  $N$ ), thereby yielding upper and lower limits on the true mid-infrared luminosity (second part of Table 2). For extremely low S/N sources, we are cannot be sure what the sizes of the sources are. We therefore performed our calculations in the limits where the sources are optically thick (blackbody limit) and optically thin (§ 3 of Table 2).

Mid-infrared luminosities were computed by integrating the Planck function from 1 to  $600 \mu\text{m}$  at the derived dust color temperature and optical depth for each source, again using the emissivity function and assuming emission into  $4\pi$  sr.

<sup>1</sup> These labels are shortened from the IAU recommended names, which are in the form Gill.II±b.bb:DPT00 #. For instance, we find that G309.92+0.48 has three mid-infrared sources, whose names in the full form are G309.92+0.48:DPT00 1, G309.92+0.48:DPT00 3 and G309.92+0.48:DPT00 2. Some sources already have names, and this will be discussed in § 4.

TABLE 1  
COORDINATES OF METHANOL MASER REFERENCE FEATURES

Target Name	R.A. (J2000)	Decl. (J2000)	Mid-IR Detection?
G305.21+0.21 .....	13 11 13.72	−62 34 41.6	N
G305.20+0.21 .....	13 11 10.47	−62 34 39.0	Y
G309.92+0.48 .....	13 50 41.76	−61 35 10.1	Y
G318.95−0.20 .....	15 00 55.40	−58 58 53.0	Y
G323.740−0.263 ...	15 31 45.46	−56 30 50.2	Y
G323.741−0.263 ...	15 31 45.88	−56 30 50.3	Y
G328.24−0.55 .....	15 57 58.38	−53 59 23.1	N
G328.25−0.53 .....	15 57 59.79	−53 58 00.9	Y
G328.81+0.63 .....	15 55 48.61	−52 43 06.2	Y
G331.28−0.19 .....	16 11 26.60	−51 41 56.6	Y
G336.43−0.26 .....	16 34 20.34	−48 05 32.5	N
G339.88−1.26 .....	16 52 04.66	−46 08 34.2	Y
G340.78−0.10 .....	16 50 14.86	−44 42 26.4	N
G345.01+1.79 .....	16 56 47.56	−40 14 26.2	Y
G345.01+1.80 .....	16 56 46.80	−40 14 09.1	Y
NGC 6334F .....	17 20 53.50	−35 47 01.7	Y
NGC 6334F-NW...	17 20 53.31	−35 46 59.7	Y
G351.44+0.66 .....	17 20 54.67	−35 45 08.5	N
G351.77−0.54 .....	17 26 42.55	−36 09 17.7	N
G9.621+0.196 .....	18 06 14.78	−20 31 32.1	N
G9.619+0.193 .....	18 06 15.04	−20 31 44.2	Y

TABLE 2  
PHYSICAL PARAMETERS DERIVED FROM THE MID-INFRARED OBSERVATIONS

Target Name	$D^a$ (kpc)	Source <sup>b</sup>	$F_{10.46 \mu\text{m}}^c$ (Jy)	$F_{18.06 \mu\text{m}}^c$ (Jy)	$T_{\text{Dust}}$ (K)	$\tau_{9.7 \mu\text{m}}^d$	$A_V^d$	$L_{\text{MIR}}$ ( $L_{\odot}$ )
Resolved Sources <sup>e</sup>								
G309.92+0.48 .....	5.4	1(m)	$52.36 \pm 0.05$	$178.53 \pm 0.32$	168	0.42	7.6	23100
		2	$2.53 \pm 0.03$	$36.66 \pm 0.33$	117	0.15	2.7	5190
G323.740-0.263 .....	3.1	1(m)	$0.37 \pm 0.02$	$3.44 \pm 0.09$	128	0.03	0.5	147
G328.25-0.53 .....	2.3	1	$0.77 \pm 0.02$	$1.80 \pm 0.10$	184	0.0025	0.05	44
		2(m)	$0.30 \pm 0.01$	$1.32 \pm 0.09$	153	0.0021	0.04	30
G339.88-1.26 .....	3.1	1(m)	$0.49 \pm 0.01$	$12.50 \pm 0.20$	105	0.13	2.4	690
		2	$0.49 \pm 0.01$	$3.00 \pm 0.10$	141	0.0026	0.05	123
G351.42+0.64 .....	1.7 <sup>f</sup>	1(m)	$64.46 \pm 0.16$	$263.59 \pm 0.73$	159	0.41	7.4	3310
		2	$11.01 \pm 0.12$	$76.23 \pm 0.41$	137	0.17	3.1	950
Unresolved Sources <sup>g</sup>								
G305.20+0.21 .....	3.9	1(m)	$28.61/34.69 \pm 0.08$	$117.53/120.80 \pm 0.29$	191/171	$\infty/1.0$	$\infty/18.1$	12700/8320
G318.95-0.20 .....	2.0	1(m)	$4.04/5.19 \pm 0.06$	$18.78/19.41 \pm 0.26$	183/161	$\infty/0.19$	$\infty/2.9$	541/337
G323.741-0.263 .....	3.1	1(m)	$0.58/0.78 \pm 0.02$	$5.44/5.62 \pm 0.10$	150/136	$\infty/0.14$	$\infty/2.5$	448/234
G328.81+0.63 .....	2.9 <sup>h</sup>	1	$3.00/3.83 \pm 0.01$	$10.00/10.36 \pm 0.12$	205/176	$\infty/0.06$	$\infty/1.1$	594/396
		2(m)	$0.73/0.94 \pm 0.01$	$12.98/13.35 \pm 0.13$	128/120	$\infty/0.79$	$\infty/14.3$	1230/552
G331.28-0.19 .....	4.8	1(m)	$0.91/1.17 \pm 0.04$	$3.27/3.39 \pm 0.18$	200/172	$\infty/0.02$	$\infty/0.4$	532/349
G345.01+1.79 .....	2.1	1(m)	$4.46/5.70 \pm 0.05$	$27.43/28.31 \pm 0.31$	168/151	$\infty/0.40$	$\infty/7.2$	918/537
G9.619+0.193 .....	0.6 <sup>i</sup>	1(m)	$0.18/0.23 \pm 0.03$	$3.56/3.66 \pm 0.18$	125/117	$\infty/0.56$	$\infty/10.1$	170/73
Unresolved, Low S/N Sources <sup>j</sup>								
G328.81+0.63 .....	2.9 <sup>h</sup>	3	$0.26/0.36 \pm 0.01$	$8.74/9.03 \pm 0.11$	112/105	...	...	1180/430
		4	$0.07/0.10 \pm 0.01$	$3.66/3.78 \pm 0.09$	102/97	...	...	678/211
		5	$0.50/0.70 \pm 0.01$	$11.05/11.42 \pm 0.19$	122/113	...	...	1170/478
		6	$0.25/0.37 \pm 0.01$	$12.10/12.50 \pm 0.20$	105/99	...	...	2050/662
G345.01+1.80 .....	2.1	1(m)	$0.18/0.23 \pm 0.02$	$0.90/0.39 \pm 0.25$	178/156	...	...	29/18
G351.42+0.64 .....	1.7 <sup>f</sup>	3	$0.05/0.08 \pm 0.01$	$6.43/6.64 \pm 0.24$	90/86	...	...	764/187
G351.77-0.54 .....	1.0 <sup>h</sup>	1	$0.16/0.21 \pm 0.03$	$1.11/1.10 \pm 0.09$	164/146	...	...	8/4
Nondetections and Sources Detected in Only One Filter								
G305.21+0.21 .....	3.9	...	<0.015	<0.197	...	...	...	...
G309.92+0.48 .....	5.4	3	$0.19 \pm 0.01^k$	<0.178	...	...	...	...
G328.24-0.55 .....	2.3	...	<0.015	<0.179	...	...	...	...
G328.25+0.53 .....	2.3	3	<0.015	$0.92 \pm 0.07^k$	...	...	...	...
G328.81+0.63 .....	2.9 <sup>h</sup>	7	$0.06 \pm 0.01^k$	<0.181	...	...	...	...
G336.43-0.26 .....	5.9	...	<0.014	<0.177	...	...	...	...
G340.78-0.10 .....	9.0 <sup>l</sup>	...	<0.015	<0.174	...	...	...	...
G351.44+0.66 .....	1.7 <sup>m</sup>	...	<0.015	DNO <sup>n</sup>	...	...	...	...
G351.77-0.54 .....	1.0 <sup>l</sup>	2	<0.016	$3.21 \pm 0.15^l$	...	...	...	...
G9.621+0.196 .....	0.6 <sup>i</sup>	...	<0.015	<0.178	...	...	...	...

NOTE—All values quotes with a “<” are upper limit flux densities at a 95% confidence level.

<sup>a</sup> All distances are adopted from Walsh et al. 1997 unless otherwise noted.

<sup>b</sup> An “(m)” denotes the sources associated with the methanol masers. Sources are labeled 1, 2, 3, etc. for each field. These are shortened from the IAU recommended names which are in the form Glllll±b.bb:DPT00 #, where # is the source number. Some of these sources already have names, as discussed in the text.

<sup>c</sup> The monochromatic flux densities are quoted here with their statistical errors. We estimate the absolute photometric accuracy for the night is ±7% for N and ±10% for IHW18.

<sup>d</sup> These values are emission optical depth at 9.7 μm and corresponding extinction in the visible.

<sup>e</sup> Value in this section are derived from our resolved sizes.

<sup>f</sup> Neckel 1978.

<sup>g</sup> Values for this section are given in the form BB/UL, where BB is the lower limit (blackbody) size of the source, and UL is the upper limit on size given by our resolution.

<sup>h</sup> MacLeod et al. 1998.

<sup>i</sup> Wink et al. 1982.

<sup>j</sup> Because of the low S/N for the sources in this section, we cannot determine they are truly resolved or not. All values for this section are given in the form BB/OT, where BB is the lower limit (blackbody) size of the source, and OT is the optically thin upper limit on size.

<sup>k</sup> Observed flux. This flux value could not be converted to a monotonic flux density because there is only flux from one filter.

<sup>l</sup> Caswell 1997.

<sup>m</sup> Norris et al. 1993.

<sup>n</sup> Did not observe this object with this filter.

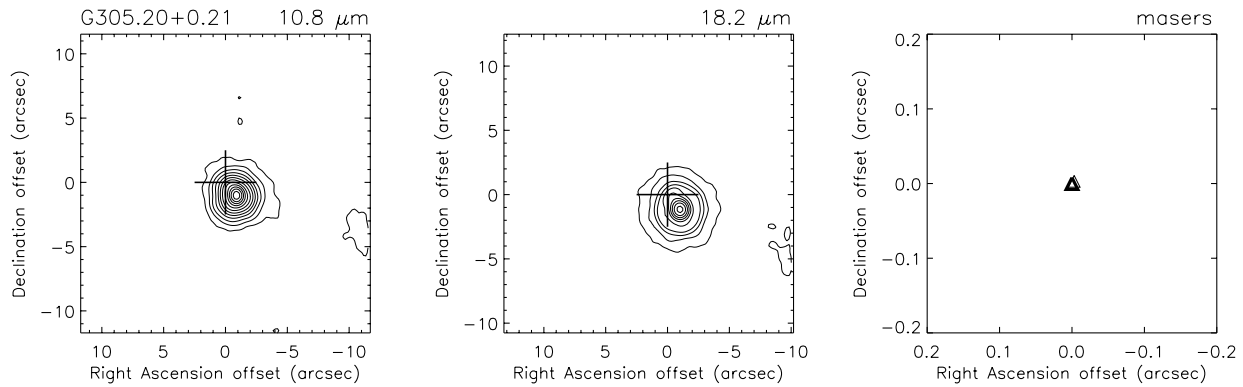


FIG. 1.—Three-panel plot of G305.20+0.21. The left panel is a contour plot of the observed  $N$ -band image, the middle panel is a contour plot of the observed IHW18 image, and the right panel is the methanol maser spot distribution of Norris et al. (1993). The crosses in the left and middle panels represent the location of the maser reference feature given by our telescopic pointing. The size of the cross depicts the estimated error in relative astrometry between the reference feature and our mid-infrared pointing. In the right panel, triangles represent 6.7 GHz methanol maser spots, and squares represent 12.2 GHz spots. The right panel is shown on a larger scale for detail.

Visual extinctions associated with the mid-infrared emitting dust were found for the sources in the survey and are listed in Table 2. These were calculated by using our derived emission optical depth values at  $9.7 \mu\text{m}$  and the Mathis (1990) extinction law, which yields the relation  $A_V = 18.09 \cdot \tau_{9.7 \mu\text{m}}$ . We find that half of the sources in our survey have  $A_V \gtrsim 2.5$  in the emitting regions. Thus, more than 90% of the visual radiation from the star is absorbed by the surrounding dust and converted into mid-infrared radiation, assuming  $4\pi$  sr coverage. However, depending on how deeply embedded the sources are, some reabsorption of the mid-infrared photons by the dust occurs, which further reprocesses them as far-infrared photons. Combined with our assumption of  $4\pi$  sr coverage, our mid-infrared luminosities derived from the mid-infrared fluxes (Table 2) can be considered reasonable lower limits to the bolometric luminosities for these sources. We used those estimates of the bolometric luminosities to estimate zero-age main sequence spectral types for the sources using the tables of Doyon (1990), which are based on stellar atmospheric models by Kurucz (1979). However, because our luminosity measurements are lower limits, the true spectral types of the sources are likely earlier than their calculated spectral types (Table 3).

#### 4. INDIVIDUAL SOURCES

In this section we review the available information for each maser site and discuss briefly the mid-infrared images we have obtained. The distances to the maser sites that are presented here are from the indicated authors with an adjustment factor applied, if applicable, to take into account the accepted distance of 8.5 kpc to the galactic center. Our adopted distances are given in Table 2.

##### 4.1. G305.21+0.21

This site contains both OH and methanol masers (Caswell, Vaile, & Forster 1995), and is located only  $22''$  to the east of G305.20+0.21. One or both of these two sites lie at the center of a large-scale CO outflow (Zinchenko, Mattila, & Toriseva 1995). The outflow is elongated predominantly east-west, extending for  $2'$ . No radio continuum emission was found from this site by Phillips et al. (1998), with an upper limit on the 8.6 GHz peak flux density of 0.5

mJy beam $^{-1}$ . Furthermore, Walsh et al. (1999) find no near-infrared source at this site in any of their passbands ( $J$ ,  $H$ ,  $K$  and  $L$ ).

Walsh et al. (1997) believe the site is located at either 3.9 or 5.9 kpc, because of confusion associated with deriving kinematic distances. Caswell & Haynes (1987b) suggest that this object lies at the near kinematic distance because the region can be seen optically. Norris et al. (1993), detected a linear distribution of four methanol masers spots from this site, with a clear monotonic spatial-velocity gradient. We were unable to detect a source at this site in either the  $N$  or IHW18 filters. Table 2 indicates our 95% confidence upper limits for a point source detection.

##### 4.2. G305.20+0.21

Figure 1 shows a strong 10 and  $18 \mu\text{m}$  detection of a single, unresolved source. This appears to be the same source observed by Walsh et al. (1999) in the near-infrared. Norris et al. (1993) describe the distribution of masers here as compact, detecting only two methanol maser spots at this site, almost coincident with each other. Like G305.21+0.21, this site contains both OH and methanol masers. Phillips et al. (1998) find no 8.6 GHz radio continuum coincident with this source with a  $0.9 \text{ mJy beam}^{-1}$  upper limit. As for G305.21+0.21, the near distance of 3.9 kpc is adopted here. This source has an unusually high emission optical depth of  $\tau = 1.0$ , giving it the highest emission optical depth for any source in our survey and also the largest optical extinction at a value of  $A_V = 18.1$ .

##### 4.3. G309.92+0.48

This site contains both OH and methanol masers, as well as radio continuum emission from an UC H II region. The OH and methanol spots are distributed along an arc that spans  $1'.1$  (Caswell 1997) and is concave to the southeast. The radio continuum peak is at the center of the arc. Norris et al. (1993) consider this site to have a well-defined velocity gradient in the 6.7 GHz methanol masers, and to be a disk candidate. Both methanol and OH spots show a velocity gradient, with increasingly negative velocities from north to south along the arc (Caswell 1997).

Walsh et al. (1997) find nine methanol maser spots at 6.7 GHz (one more than Norris et al. 1993) lying at a tangent

TABLE 3  
THE NATURE OF THE SOURCES ASSOCIATED WITH METHANOL MASERS

Name	Linear Masers?	IR Detections	Mid-IR Morphology <sup>a</sup>	Radio Continuum Flux <sup>b</sup> (mJy)	Radio Spectral Type <sup>c</sup>	Mid-IR Spectral Type <sup>d</sup>
Mid-Infrared Sources Without Radio Continuum						
G305.20+0.21:DPT00 1 .....	no	H, K, L, N, IHW18	C, S	<0.9	<B2.7	B1.6
G318.95-0.20:DPT00 1 .....	yes	H, K, L, N, IHW18	C, S <sup>e</sup>	<0.7	<B3.6	B6.9
G323.740-0.263:DPT00 1 .....	yes	L, N, IHW18	C, E	<0.2	<B3.8	B8.3
G323.741-0.263:DPT00 1 .....	no	H, K, L, N, IHW18	C, S	<0.2	<B3.8	B7.5
G328.25-0.53:DPT00 2 .....	no	K, L, N, IHW18	E(L)	<0.6	<B3.5	A1.5
G345.01+1.80:DPT00 1 .....	yes	L, N, IHW18	C(L)	<0.7	<B3.5	A3.7
G351.42+0.64:DPT00 3 .....	no	N, IHW18	E(L)	<6.3	<B2.7	B7.9
Mid-Infrared Sources With Radio Continuum						
G309.92+0.48:DPT00 1 .....	yes	H, K, L, N, IHW18	C,E	351	B0.3	B0.7
G328.81+0.63:DPT00 2 .....	yes	NEAR <sup>f</sup> , N, IHW18	?	1640 <sup>g,h</sup>	?	B5.8
G331.28-0.19:DPT00 1 .....	yes	N, IHW18	C,S <sup>e</sup>	4.1	B2.1	B6.8
G339.88-1.26:DPT00 1 .....	yes	H, K, L, N, IHW18	E	14 <sup>i</sup>	B1.9	B5.4
G345.01+1.79:DPT00 1 .....	yes	L, N, IHW18	C <sup>j</sup>	260 <sup>g</sup>	B0.9	B5.9
G351.42+0.64:DPT00 1 .....	no	H, K, L, N, IHW18	E	2780	B0.4	B2.5
G9.619+0.193:DPT00 1 .....	no	N,IHW18	C,S	92	B1.5	A0.2
Radio Continuum Sources Without Mid-Infrared Continuum						
G328.24-0.55 .....	no	DNO <sup>k</sup>	...	27	B1.9	...
G340.78-0.10 .....	no	...	...	9 <sup>g</sup>	B1.1	...
G351.77-0.54 .....	no	K, L	...	3 <sup>l</sup>	B2.7	...
G9.621+0.196 .....	no	...	...	6	B2.6	...
Sources Without Radio Continuum and Without Mid-Infrared Continuum						
G305.21+0.21 .....	yes	...	...	<0.5	<B3.0	...
G336.43-0.26 .....	yes	...	...	<0.3	<B2.9	...

NOTE—A question mark indicates that a value or property cannot be ascertained owing to confusion.

<sup>a</sup> Morphology of closest mid-infrared source to the methanol masers given our astrometry: C = compact, S = symmetric, E = elongated, (L) = low signal-to-noise.

<sup>b</sup> All values are integrated 8.5 GHz flux densities from Phillips et al. 1998, unless otherwise noted. All “<” symbols denote peak radio flux density upper limits.

<sup>c</sup> From the values and upper limits on radio continuum flux given in this table, and the distances to the sources given in Table 2, we derived Lyman photon rates from the standard equation for free-free emission, assuming an electron temperature of 10,000 K and Case B recombination. We then used the tables of Doyon 1990 to find the spectral type corresponding to our derived Lyman photon rate.

<sup>d</sup> Derived from mid-infrared luminosities in Table 2. For unresolved sources, spectral types were derived from the luminosities stated in the optically thin case.

<sup>e</sup> PSF star for this observation appeared elongated at the same position angle.

<sup>f</sup> NEAR denotes a detection in the near-infrared, but there is confusion caused by multiple sources and a foreground star which do not permit accurate near-infrared flux density estimates.

<sup>g</sup> Caswell 1997, 6.7 GHz.

<sup>h</sup> The radio flux may not be coming from the source associated with the maser emission.

<sup>i</sup> Ellingsen et al. 1996, 8.6 GHz.

<sup>j</sup> The image of G345.01+1.79:DPT00 1 appears elongated at a position angle of 25°, however the PSF observation for this source is elongated as well, but at a position angle of ~0°. Given that the elongations are at different angles, it is not certain if the elongation of G345.01+1.79:DPT00 1 is real.

<sup>k</sup> DNO means that the source was not observed in the near-infrared.

<sup>l</sup> Fix et al. 1982, 5 GHz.

point distance of 5.4 kpc, which is slightly different than the distance of 4.7 kpc adopted by Norris et al. (1993). Walsh et al. (1997) also conclude that if the region were powered by a single star, it would have to be an O5.5 star with a luminosity of  $3.1 \times 10^5 L_{\odot}$  in order to explain the FIR radiation observed by *IRAS*.

Walsh et al. (1998) report methanol maser positions that are offset 1" from those of Norris. They also conclude that the methanol masers are slightly offset (0".1) from their 8.64 GHz continuum peak. Their radio continuum observations show an azimuthally symmetric UC H II region. Phillips et al. (1998) observed the same UC H II region with an integrated flux density of 676 mJy.

Our mid-infrared observations (Fig. 2b) show two resolved sources (1 and 2) at a position angle of 53°, both seen

at 8.6 GHz by Phillips et al. (1998) and in the near-infrared by Walsh et al. (1999). A third source that is only seen in the mid-infrared in *N*-band to the west (Fig. 2a), has no associated radio continuum, but is seen in the near-infrared by Walsh et al. (1999). At 18.2  $\mu$ m, the central peak of source 1 is clearly arc-shaped and concave to the northwest in the opposite sense in comparison with the methanol masers.

Relative astrometry between the radio continuum sources and masers in Phillips et al. (1998) is stated as being better than 0".3. Assuming radio continuum peaks are coincident with mid-infrared peaks, we registered our mid-infrared images with those of Phillips et al. (1998) to obtain more accurate relative astrometry between the mid-infrared source 1 and maser positions (Fig. 2b). This technique yielded the result that the mid-infrared arc is located just

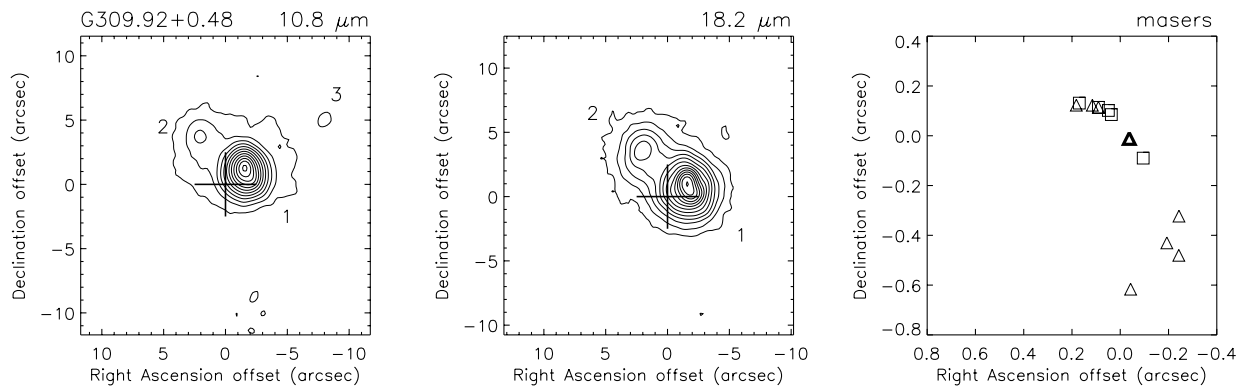


FIG. 2a

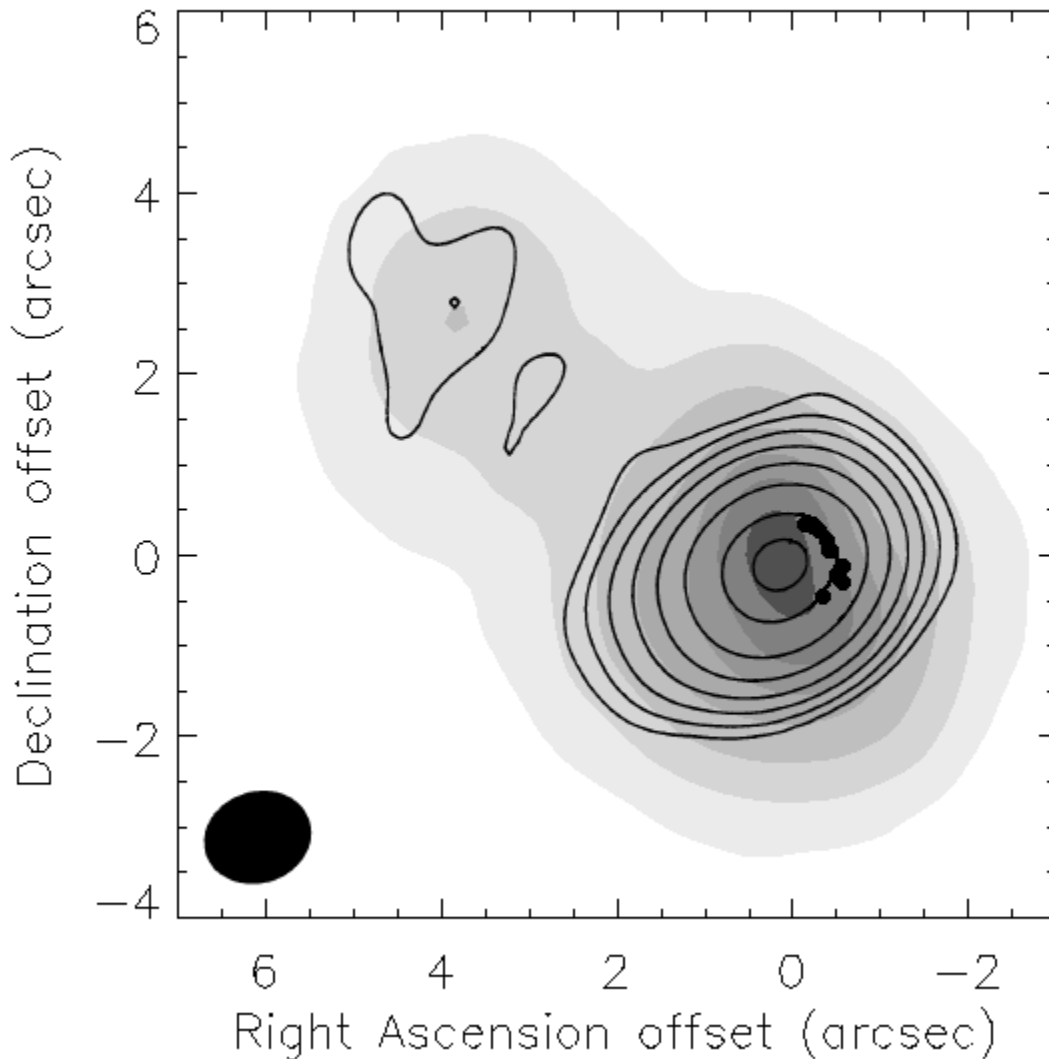


FIG. 2b

FIG. 2.—(a) Same caption as Fig. 1, but for G309.92+0.48. Source 1 is elongated and arced in an opposite sense as the masers. (b) A filled contour plot of the IHW18 image with the 8.6 GHz radio continuum image of Phillips et al. (1998) overlaid. The radio continuum peak was assumed to be coincident with the mid-infrared peak. Methanol masers are shown as filled circles. The size of the Gaussian restoring beam is shown in the lower left of the plot.

southeast of the maser arc, and that they have similar extent.

There are two possible explanations for the nature of G309.92+0.48:DPT00 1. Since the masers are slightly offset from the radio continuum peak and follow the curves along

the contours of constant intensity, it is plausible that they might be tracing a shock associated with the expanding UC H II region. An alternate explanation is that the arcs of methanol and thermal emission seen in Figure 2b extending from the northeast to the southwest may be tracing out a

nearly edge-on flared disk. The northwest pole of the rotation axis would have to be tilted slightly away from us. In the mid-infrared, we would view the warm emission associated with the irradiated disk surface. If the disk is optically thick to mid-infrared radiation we would only see the part of the disk within our direct line of sight and it would appear as an arc. The maser photons, on the other hand, are coming to us through the flared edge of the disk closest to us, where the line of sight is unobscured at radio wavelengths. We do not see any maser photons beamed to us from the far side of the disk, because they would have to travel through the H II gas below the disk, and would be absorbed.

#### 4.4. G318.95–0.20

Methanol masers were discovered at this site by Kembell, Gaylard, & Nicolson (1988) at the 12.2 GHz transition. Norris et al. (1993) show this site to have a linear distribution of seven methanol masers with a reasonable velocity gradient along them (Walsh et al. 1997 found 11 spots).

Walsh et al. (1997) find that the source may lie at kinematic distances of either 2.0 kpc or 10.9 kpc. Caswell et al. (1995) believe that the larger distance is more likely because they find no optical counterpart to this object. However, if this is the case, G318.95–0.20 would have one of the largest maser luminosities known to date (97,000 Jy kpc<sup>2</sup>). Furthermore, given that the sources in our survey are highly embedded, we would not expect to detect anything in the optical. Phillips et al. (1998) detect no 8.5 GHz continuum detected at this site, with an upper limit peak flux density of 0.7 mJy beam<sup>-1</sup>.

Ellingsen, Norris, & McCulloch (1996) estimate this to be the site of a star with a spectral type later than B2, as derived from their upper-limit nondetection of radio continuum at 8.5 GHz, and using a distance of 2.0 kpc. We find a single mid-infrared source coincident with the near-infrared source seen by Walsh et al. (1999), which is slightly elongated in the north-south direction, similar to the position angle of the maser spots (source 1, Fig. 3). However, this source looks similar to the PSF star imaged near this position, and consequently the elongation in the source may not be real.

#### 4.5. G323.740–0.263 and G323.741–0.263

Like G318.95–0.20, Kembell et al. (1988) were the first to discover methanol masers at this location in the 12.2 GHz transition. This site contains two maser groups

separated by 3".5 (Phillips et al. 1998). The western grouping, G323.740–0.263, is the same observed by Norris et al. (1993), and the eastern maser grouping, G323.741–0.263, contains four maser spots distributed nonlinearly. Because of the seemingly nonlinear distribution of the western group of methanol masers, it is categorized as complex by Norris et al. (1993). The spots of G323.740–0.263 are not evenly distributed in a line or arc, and there is no clear velocity gradient. However, there may be two distinct lines of methanol masers crossing each other. Most points can be fit by two lines, with one at a position angle of  $\sim 300^\circ$ , and the other  $\sim 20^\circ$ .

Walsh et al. (1997) determined the distance to be 3.1 or 10.9 kpc. Based upon the *IRAS* FIR fluxes, they determine that a single star would have a luminosity of  $5.0 \times 10^4$  or  $6.3 \times 10^5 L_\odot$ , with a spectral type of O8.5 or O5, respectively, for the two given distances. Phillips et al. (1998) detect no radio continuum in this area with a  $4\sigma$  upper-limit peak flux density of 0.2 mJy beam<sup>-1</sup>.

Our observations of this site reveal a double source in the mid-infrared (Fig. 4a), also imaged by Walsh et al. (1999) in the near-infrared. The western source, which Walsh et al. (1999) detected only at *L*, is resolved and elongated in the mid-infrared at the same position angle as the line of masers ( $300^\circ$ ) in G323.740–0.263. We point out that a majority (12 of 17) of the 6.7 and 12.2 GHz methanol masers observed by Norris et al. (1993) at this site lie along the  $300^\circ$  line. The two distinct sites of methanol masers found by Phillips et al. (1998) have relative offsets similar to the offsets between the two mid-infrared sources (Fig. 4b). We can therefore say with confidence that the line of masers in G323.740–0.263 is coincident with our elongated western source, in both location and position angle. The masers along this line may trace out a circumstellar disk, while the other remaining masers at the position angle of  $\sim 20^\circ$  may be associated with an outflow (Phillips et al. 1998). The eastern mid-infrared source is unresolved. It lies 3" away from the western source, which places the G323.741–0.263 masers seen by Phillips et al. (1998) just outside the mid-infrared contours of the eastern source. This maser group may exist in an outflow associated with the eastern source.

#### 4.6. G328.24–0.55

This site lies approximately 82".5 south and 13".0 west of G328.25–0.53, and is assumed to be at the same kinematical distance. Walsh et al. (1997) determined the distance

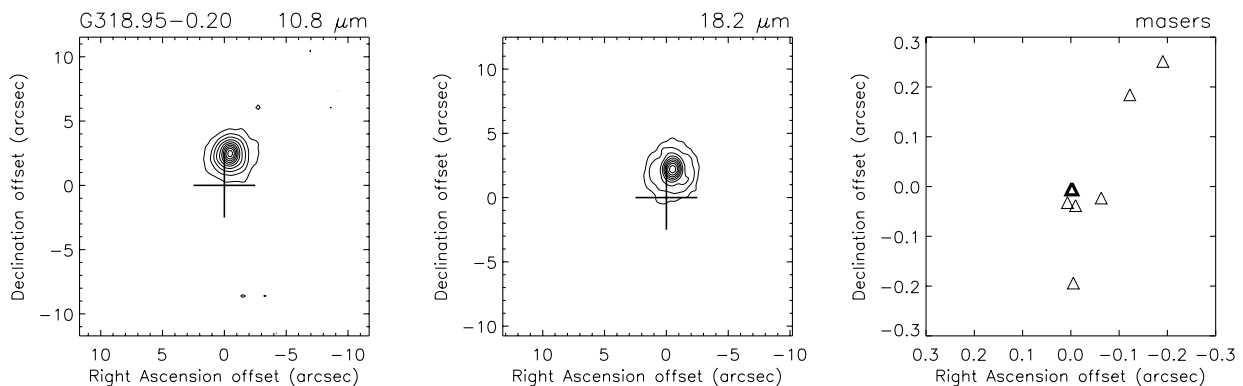


FIG. 3.—Same as Fig. 1, but for G318.95–0.20. The source appears elongated in the north-south direction, similar to the maser distribution. However, the PSF for this source is elongated in the same direction, and therefore the source elongation is most likely not real.

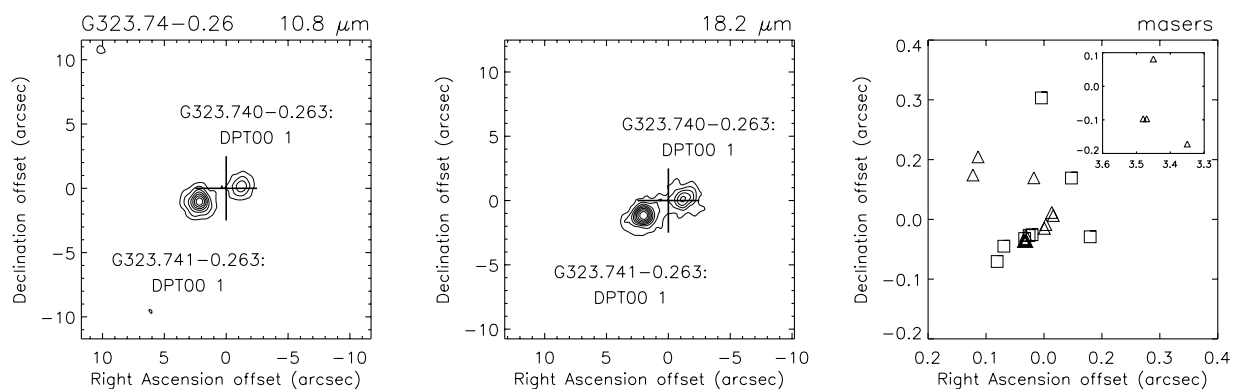


FIG. 4a

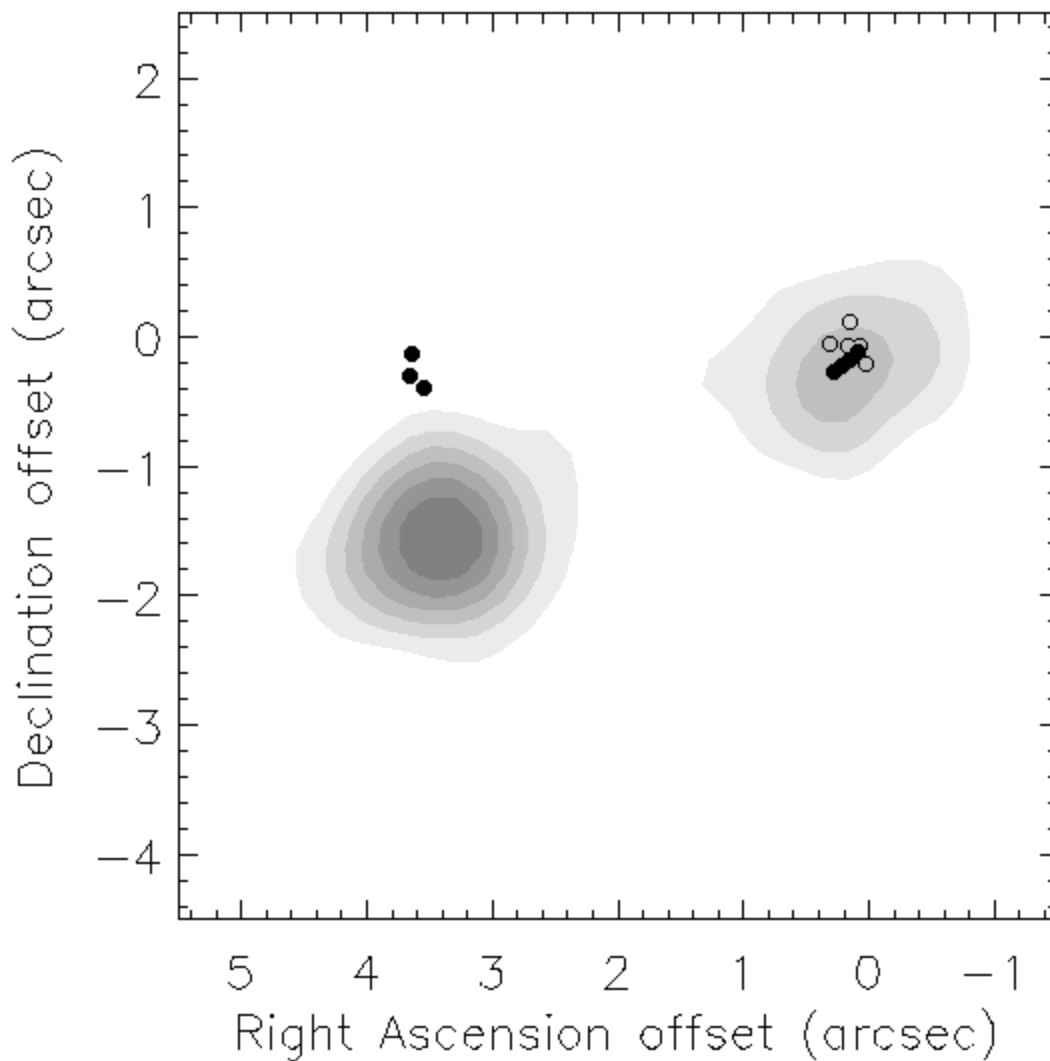


FIG. 4b

FIG. 4.—(a) Same as Fig. 1, but for G323.74–0.26. This site contains both G323.740–0.263 and G323.741–0.263. The right panel displays the maser distribution for G323.740–0.263, and the inset shows the masers of G323.741–0.263 that lie  $\sim 3''.5$  to the east of G323.740–0.263. (b) A filled contour plot of the IHW18 image with the methanol masers overlaid as circles. The methanol masers in the western group were assumed to be coincident with the elongated western mid-infrared source, G323.740–0.263:DPT00 1. To more clearly show the line of methanol masers associated with this source, the masers not in the linear distribution are shown as open circles. These may be tracing an outflow. The masers associated with the eastern mid-infrared source G323.741–0.263 may also be tracing an outflow.

to the source to be 2.3 or 12.1 kpc, which generally agrees with Caswell et al. (1995) (2.6/11.8 kpc). Again Caswell et al. (1995) favor the larger distance because there is no optical counterpart, although Norris et al. (1993) use the smaller value. The methanol spots are not distributed linearly, and according to Norris this source does not show a well-defined velocity gradient along the spots. Phillips et al. (1998) detect an 8.6 GHz continuum source at the location of the methanol masers with an integrated flux density of 27.7 mJy. Phillips et al. (1998) suggest, among other scenarios, that since the masers are distributed in two clumps lying on either side of the UC H II region they may be tracing the two edges of a circumstellar disk, or two sources in a binary. We, however, were unable to detect a mid-infrared source at this location with a  $3\sigma$  upper limit on point source flux densities of 15 mJy at  $N$  and 179 mJy at IHW18.

#### 4.7. G328.25–0.53

Walsh et al. (1997) find five masers at this site (same as Norris et al. 1993) and infer from the *IRAS* FIR flux that this area would contain a star with a luminosity of  $4.3 \times 10^4$  or  $1.2 \times 10^6 L_{\odot}$ , depending on the assumed kinematical distance (see G328.24–0.55). This corresponds to a spectral class of O9 or O4, respectively (Panagia 1973).

Phillips et al. (1998) detect no 8.6 GHz radio continuum at this site with an upper limit of  $0.6 \text{ mJy beam}^{-1}$ . We detect two elongated low S/N sources at  $N$ , both of which are seen in the near-infrared by Walsh et al. (1999). There is an additional source only seen at IHW18. The IHW18 detections are even lower S/N than the  $N$ -band detections (Fig. 5). Using our astrometry alone, it is not clear which of the three sources the masers are associated with even though our pointing places them closest to source 2. However, the near-infrared imaging of Walsh et al. (1999) seems to confirm the association of the methanol masers with the source corresponding to our mid-infrared source 2.

The five methanol masers are not distributed in a single line, but are in two tight groups separated by  $0''.8$ , and are not considered linearly distributed by Norris et al. (1993). Source 2 is elongated at a position angle of  $\sim 30^\circ$ , and interestingly the western group of three masers are best fitted with a regression line at an angle of  $27^\circ$ . One possibility is that the three masers are tracing a disk, and the other two masers could be excited by an outflow or other stellar process. However, we do not consider a maser grouping to be linear in this paper unless there are at least four

points in the linear distribution. We furthermore do not know where exactly the methanol masers are with respect to source 2, and they may not be exactly coincident with our mid-infrared source.

#### 4.8. G328.81+0.63

This site contains OH and methanol masers, as well as prominent radio continuum emission (Caswell 1997). Caswell (1997) believes that there are perhaps two separate sites of maser emission, however they are only separated by 30 mpc, and the velocity ranges of the masers overlap. This site contains OH masers at the 1612, 1665, and 1667 MHz transitions (Caswell, Haynes, & Goss 1980), as well as the 1720 MHz (MacLeod et al. 1998) and 6.035 GHz OH maser transitions (Caswell & Vaile 1995). Methanol masers have been seen at both the 6.7 GHz transition (MacLeod, Gaylard, & Nicolson 1992; Norris et al. 1993) and 12.2 GHz transition (Norris et al. 1987). Though the methanol masers are distributed in a linear fashion, Norris et al. (1993) point out that there is no coherent velocity gradient along the spots. The OH and methanol masers at this site are intermingled spatially. Walsh et al. (1997) and Caswell et al. (1995) detected six methanol masers from this region (Norris et al. 1993 found eight).

Caswell (1997) and Norris et al. (1993) both believe this source to be located at 2.6 kpc away. MacLeod et al. (1998) made formaldehyde measurements that lead to a near distance of 2.9 kpc, and a far distance of 11.7 kpc. These values are consistent with the near and far values given by Walsh et al. (1997) (3.2/13.6 kpc). Caswell et al. (1995) claim they prefer their larger kinematic distance of 11.9 kpc, because the site lacks an optical counterpart, but again, this is likely due to large extinction at optical wavelengths. It would seem that the near distance is probably the correct distance given the argument of Caswell (1997), who states that the far kinematic distance is unlikely in this case because the source is greater than  $0.5^\circ$  from the Galactic plane.

Caswell (1997) categorizes this as one of the brightest “steep-spectrum” sources in the *IRAS* Point Source Catalog, and it may represent an early epoch in the formation of a massive star. Caswell also observed G328.81+0.63 in 6 cm radio continuum. Using the *IRAS* FIR fluxes and a distance of 2.9 kpc, Caswell estimates the spectral type of a single star in this area to be an O6.3, and using the 6 cm data finds a spectral type of O9.3. Walsh et al. (1997) concluded that the *IRAS* FIR flux would yield a  $2.69 \times 10^5 L_{\odot}$  star with a spectral type of O6, if there were only one star

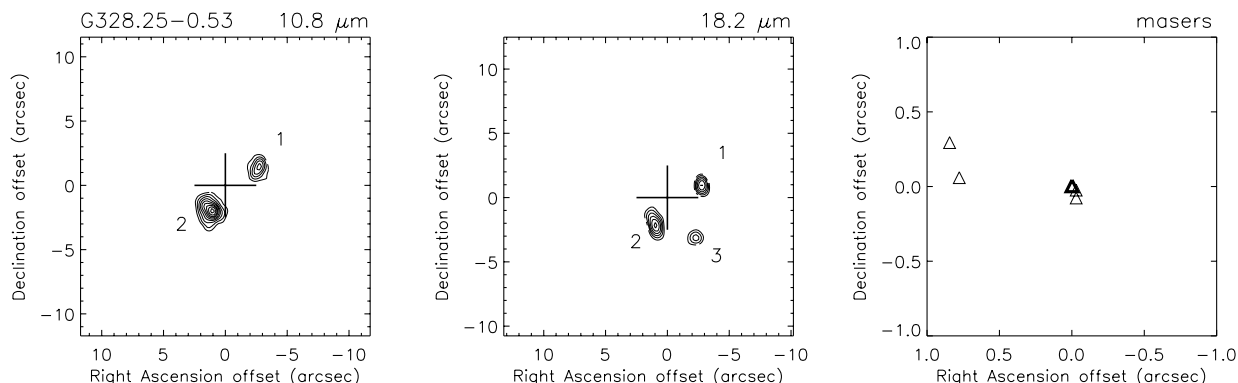


FIG. 5.—Same as Fig. 1, but for G328.25–0.53. All three sources have low signal-to-noise. Sources 1 and 2 are resolved and elongated. Source 2 is most likely the mid-infrared source associated with the methanol masers.

responsible for the flux in this region. This is consistent with the findings of Caswell (1997).

Caswell (1997) finds an extended H II region with a flux density of 2 Jy, and an unresolved companion UC H II region with a flux density of 360 mJy  $\sim 3''$  to the east. Walsh et al. (1998) detects both the compact and extended H II regions observed by Caswell (1997). Their astrometry places the maser group to the west coincident with the extended H II region peak, and the smaller maser group to the east coincident with the unresolved UC H II region. Osterloh, Henning, & Launhardt (1997) present a  $K'$  (2.15  $\mu\text{m}$ ) image of this area. They determine it to be an embedded cluster of fewer than four stars sitting behind a foreground star, which precludes them from assigning the objects accurate  $K'$  fluxes. They also find evidence for CO outflow using the deviation from the Gaussian profile in the CO(2  $\rightarrow$  1) line.

Even contaminated with a foreground star in the  $K'$  image, the near-infrared image of G328.81+0.63 looks similar to our mid-infrared images. However, with our observations having a factor of 3 better resolution than the  $K'$  image and no foreground star, we can distinguish six separate objects in the IHW18 image (Fig. 6a). All six sources are not as prevalent in the  $N$ -band image (consistent with the *IRAS* steep-spectrum). The two brightest sources (1 and 2 in Fig. 6a) are close to each other but resolved (and perhaps a binary), and are coincident with the confused source at  $K'$  of Osterloh et al. (1997). We again used the technique of registering our mid-infrared images with radio maps (as described in § 4.3) to achieve better relative astrometry between the mid-infrared sources and maser positions. In this case we used the radio maps of Walsh et al. (1998), and conclude that members of the western group of masers overlap the mid-infrared peak of source 2 (our mid-infrared pointing was poor, as seen in Fig. 6), and are distributed at a similar position angle to that of the sources 1 and 2 (Fig. 6b). Sources 1 and 3 match the radio contours of the extended H II region seen by Walsh et al. (1998). However, we do not detect any object at the location of the compact H II region to the east, and it seems there is either a suppression or no radio continuum emission whatsoever associated with our source 2.

#### 4.9 G331.28–0.19

This site, according to Caswell et al. (1995), is one of the few maser sites where the strength of the 12 GHz methanol masers rival that of the 6.7 GHz. Norris et al. (1993) find no coherent velocity gradient along the maser spots, though they are linearly distributed. Whereas Norris et al. (1993) found nine 6.7 GHz methanol maser sources, Walsh et al. (1997) has found 12.

Walsh et al. (1997) find that the sources lie at either 4.8 or 10.1 kpc. Norris et al. (1993) use the shorter distance, though they determined this distance to be 4.1 kpc. If this site lies at the distance of 4.8 kpc, Walsh et al. (1997) derive a luminosity of  $1.9 \times 10^5 L_{\odot}$  for a single star, which would be a spectral class of O6.5. At the larger distance, a single star would have a luminosity of  $8.5 \times 10^5 L_{\odot}$  and have a spectral type of O5.

Henning, Chan, & Assendorp (1996) find this to be a site of an interesting 21  $\mu\text{m}$  emission feature, as determined from *IRAS* LRS (Low-Resolution Spectrometer) spectra. It is not known what the carrier of the 21  $\mu\text{m}$  feature is, although the most accepted theories at present are that they are due to PAHs (polyaromatic hydrocarbons) or PAH

clusters (Hrivnak, Kwok, & Geballe 1994; Omont et al. 1995) or the inorganic substance  $\text{SiS}_2$  (Goebel 1993). However, we caution that the LRS confusion limit is  $6'$ , and these spectra may have very little to do with the source directly associated with the methanol masers.

Phillips et al. (1998) find an amorphous 8.6 GHz continuum source (poorly imaged owing to lack of short baselines for this observation) at the location of the masers with an integrated flux density of 4.1 mJy. Our mid-infrared images (Fig. 7) only show one source, which is very slightly elongated north-south at a similar position angle as the methanol masers. However, the PSF for this object appears similarly elongated and comparable in extent. We conclude that this mid-infrared source is unresolved. It is also not clear if the masers or the radio continuum source are directly associated with this mid-infrared source, given the fact that they are over  $4''$  west of the mid-infrared pointing center. Walsh et al. (1999) also fails to detect a source in the near-infrared coincident with the masers, but finds an elongated source  $\sim 2''$  to the west. This elongated near-infrared source may be associated with the source we are seeing in the mid-infrared.

#### 4.10 G336.43–0.26

Norris et al. (1993) find this site to contain five 6.7 GHz methanol masers arranged in an arc and displaying a strong systematic velocity gradient. However, Caswell et al. (1995) and Walsh et al. (1997) find eight methanol maser spots in all. Caswell et al. (1995) also did not find any evidence for OH emission from this area. Furthermore, Phillips et al. (1998) detect no 8.6 GHz continuum here at a flux density limit of  $0.3 \text{ mJy beam}^{-1}$ .

Walsh et al. (1997) determined the distances to this site to be either 5.9 or 9.9 kpc. They give no estimate of the luminosity or spectral types for a single star at these distances because the FIR fluxes from *IRAS* are only given as upper limits. Walsh et al. (1999) do not detect any near-infrared source coincident with the masers. Likewise, we do not see any sources at this location and can only provide upper limit flux densities of 14 mJy for  $N$ -band and 177 mJy for IHW18 with a confidence level of 95%.

#### 4.11 G339.88–1.26

Ellingsen et al. (1996) produced the first radio continuum image of this site at 8.5 GHz with an integrated flux density of 14 mJy. Their image is mostly unresolved but does show some extension in the northeast direction, which they suggest may be a UC H II region with a cometary morphology. In contrast, Walsh et al. (1998) present 8.6 GHz radio maps of the region showing a just unresolved, almost circular source. However, there are slight elongations in the northeast and northwest directions.

Ellingsen et al. (1996) consider this to be one of the strongest sites of methanol maser emission at both 6.7 and 12.2 GHz. The maser spots of Norris et al. (1993) lie across the radio source almost perpendicular to the position angle of the continuum extension. Two OH masers are known to straddle the methanol masers in both the north-south and east-west directions (Caswell et al. 1995). An  $\text{H}_2\text{O}$  maser is also known to exist  $\sim 1''$  south of the methanol masers (Forster & Caswell 1989).

Caswell et al. (1995) and Walsh et al. (1997) find there to be 12 6.7 GHz methanol masers here, whereas Norris et al. (1993) finds only eight. Norris et al. (1993) show this source

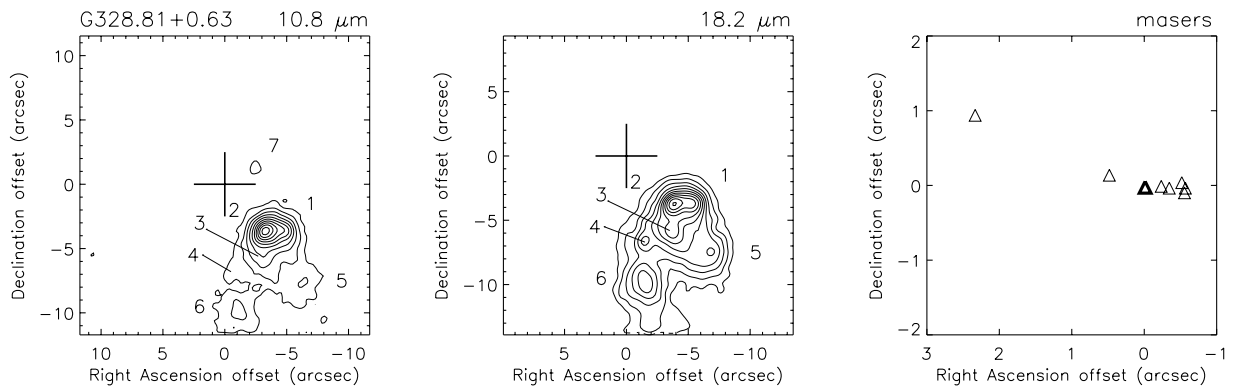


FIG. 6a

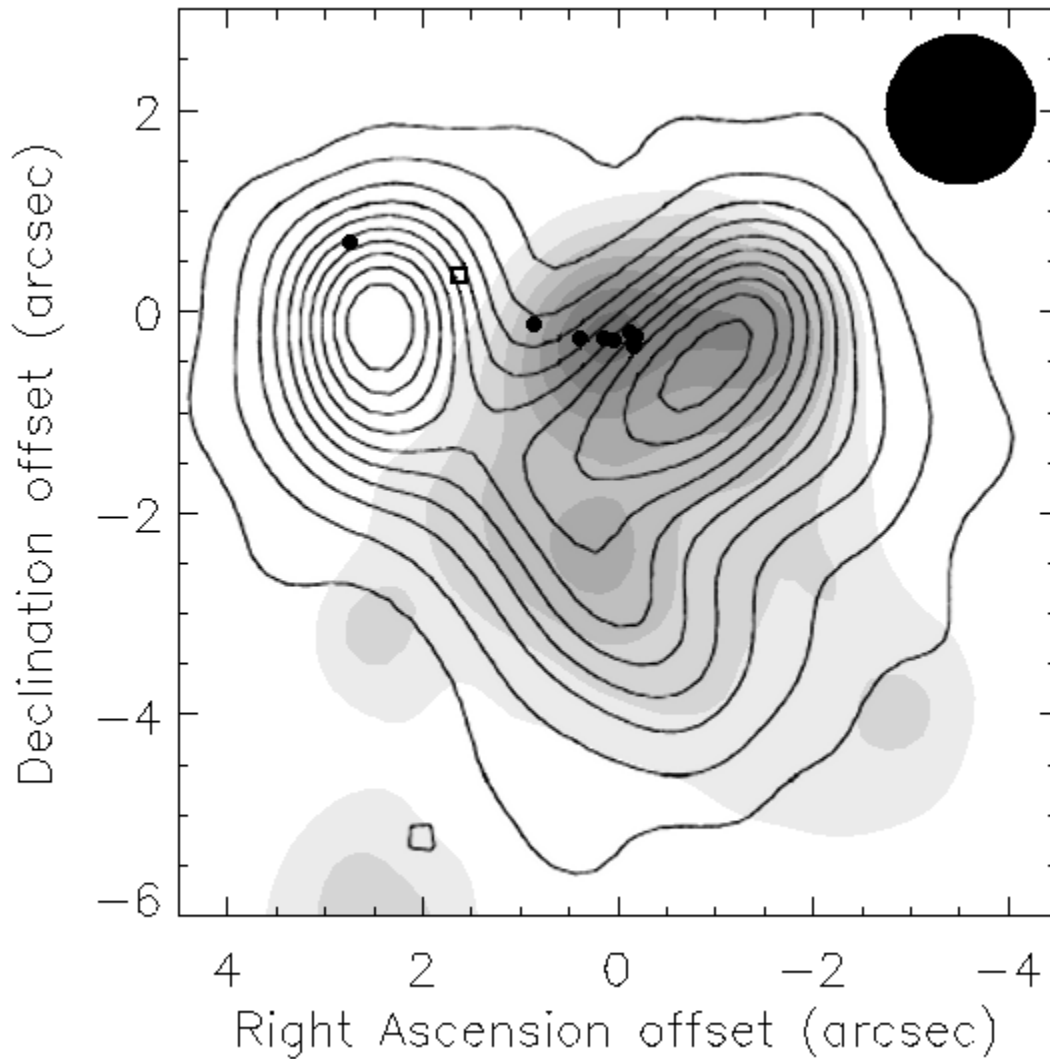


FIG. 6b

FIG. 6.—(a) Same as Fig. 1, but for G328.81+0.63. (b) By overlaying the 8.6 GHz radio continuum image of Walsh et al. (1998) and assuming the radio continuum contours to be coincident with the mid-infrared contours, we find that our astrometry in Fig. 6a was off by almost 5". The radio map traces our sources 1 and 3 well but shows no signs of source 2. Instead there is radio emission from an unresolved source to the east that we do not see in the mid-infrared. Methanol masers are shown as filled circles. The methanol masers are distributed linearly over the mid-infrared peak of source 2. The open square is an OH maser from Caswell et al. (1995). The size of the Gaussian restoring beam for the radio continuum is shown in the upper right of the plot.

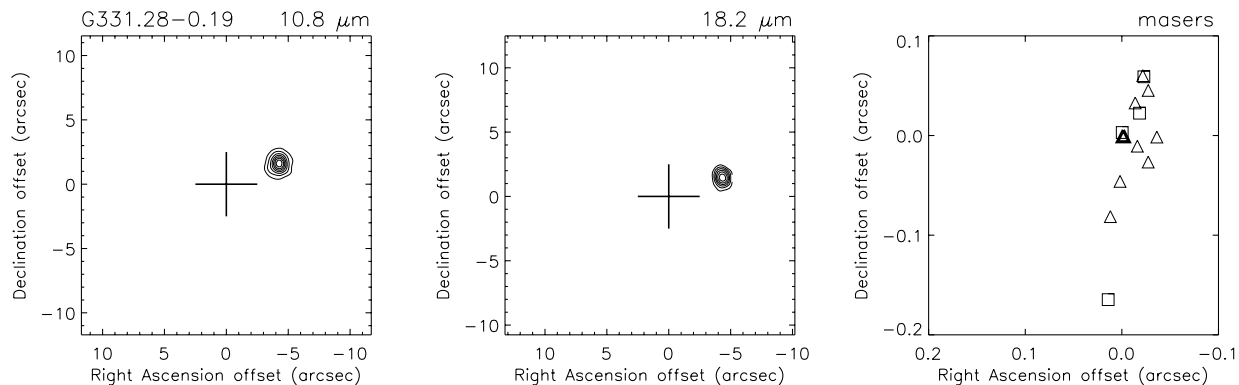


FIG. 7.— Same as Fig. 1, but for G331.28–0.19. The source appears elongated in the north-south direction, similar to the maser distribution. However, the PSF for this source is elongated in the same direction, and therefore the source elongation is not real.

to have a velocity gradient (except for maser spot a) in the 6.7 GHz masers, whereas at 12.2 GHz there is no clear velocity gradient. Walsh et al. (1997) determine the distance to this site to be either 3.1 or 12.9 kpc, and since the Galactic latitude is greater than  $0^{\circ}5$ , the near value is adopted here. If this site were to contain only one star, *IRAS* FIR fluxes would lead to a luminosity of  $8.0 \times 10^4 L_{\odot}$  or  $1.4 \times 10^6 L_{\odot}$ , with spectral types of O7.5 or earlier than O4, depending on distance.

This site was first imaged at  $10 \mu\text{m}$  by the TIMMI instrument at the ESO 3.6 m telescope in 1998 March by Stecklum & Kaufl (1998). They found a  $10 \mu\text{m}$  source and assume that this is a circumstellar disk because of the elongation they observe, combined with the apparent coincidence of the position angles of the elongation and the methanol maser linear distribution. This elongation is also observed by Walsh et al. (1999) in the *L*-band. Our observations show this site to contain at least two sources in the mid-infrared (Fig. 8a, sources 1 and 2). The more northerly source, 1, is the source imaged by TIMMI and Walsh et al. (1999), but actually may be a double source, appearing clearly elongated in the northwest direction at *N*, and appearing as two components at IHW18. Figure 8b shows the radio continuum of Ellingsen et al. (1996) and the methanol masers overlaying the mid-infrared filled contour map of source 1 at *N*. We assumed here that the radio peak coincides with the peak at *N*. It is clearly seen that the elongation in the infrared is similar to the position angle of the distribution of methanol masers. Furthermore, the ionized gas is elongated in a direction almost perpendicular to the mid-infrared elongation, perhaps tracing an outflow.

#### 4.12. G340.78–0.10

This is a site of OH masers, as well as methanol, and also contains a weak (9 mJy) UC H II region at 6.0 GHz detected for the first time by Caswell (1997). The OH and methanol masers found here overlap spatially and in velocity as well. Caswell (1997) observed this site over a larger velocity range than Norris et al. (1993), and observed more methanol maser spots. Caswell (1997) found this location to contain the largest velocity spread ( $-112$  to  $-86 \text{ km}^{-1}$ ) of any known maser site. Later observations by Phillips et al. (1998) confirm this velocity range, and resolve 19 maser spots. They also detect the weak UC H II region seen by Caswell (1997). It is argued by Caswell (1997) that the kinematic distance to this site is unambiguously 9 kpc,

because the systemic velocity of the region indicates a location near the tangent point.

The methanol maser spot morphology is very complex. It appears that the masers lie in two distinct lines: one north-south and one east-west, all contained within 1 arcsec<sup>2</sup>. Caswell (1997) suggests that this might be the site of two stars surrounded by two toroids. Features in the north-south line within the velocity range of  $-92$  and  $-86 \text{ km}^{-1}$  have a velocity field more indicative of outflow, rather than rotation. Norris et al. (1993) do not find any significant velocity gradient in either of the two linear maser structures.

Like the near-infrared survey of Walsh et al. (1999), our mid-infrared observations yielded no detection of any sources. An upper limit on the point source flux density of an *N*-band source is 15 mJy and 177 mJy for IHW18 with a 95% level of confidence.

#### 4.13. G345.01+1.79

This site has methanol and OH masers, and is coincident with an UC H II region (Caswell 1997; Caswell et al. 1995). Walsh et al. (1997) determine the distance to this site to be either 2.1 or 14.5 kpc. This is in fair agreement with Caswell (1997), who derives distances of 2.6 and 13.9 kpc. Since the Galactic latitude is greater than  $0.5^{\circ}$ , the near value of Walsh et al. (1997) is adopted here. Using the distances of Walsh et al. (1997), this would yield a single star of  $8.5 \times 10^4$  or  $4.0 \times 10^6 L_{\odot}$ , and a corresponding spectral type of O7.5 or less than O4, depending on which distance was chosen.

The methanol masers here are distributed in a linear fashion and show a moderately systematic velocity gradient among the spots (Norris et al. 1993). They seem to be offset from the peak of the radio continuum by approximately  $0^{\circ}5$  to the west. The UC H II region has an integrated flux density of 260 mJy (Caswell 1997). Walsh et al. (1998) confirm the displacement of the masers with their 8.6 GHz radio map of the area and conclude that the masers extend radially with respect to the circular UC H II region. These masers could be indicative of outflow. The two OH masers lie above and below the methanol maser distribution.

Walsh et al. (1999) observed this site in the near-infrared and find a single source visible only at *L*. We find a single bright mid-infrared source (Fig. 9) coincident with the near-infrared source that may be marginally resolved at IHW18. It appears slightly elongated in the northeast direction, at a position angle that differs from the methanol maser position angle by about  $50^{\circ}$ . However, the two OH masers lie at

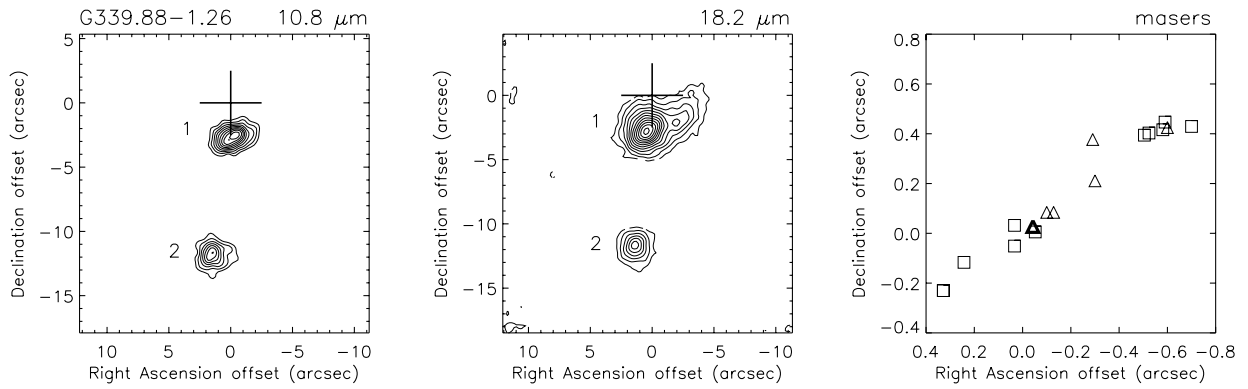


FIG. 8a

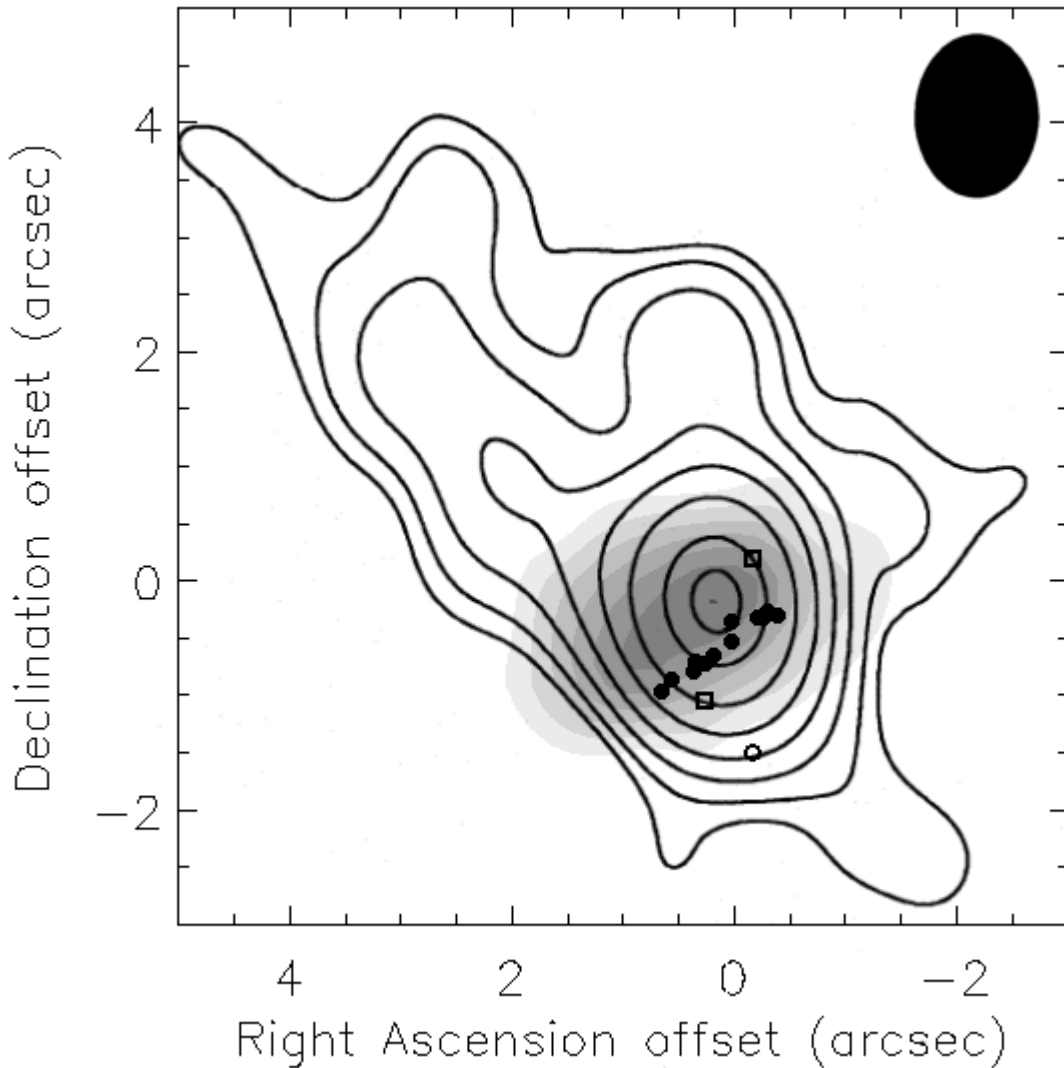


FIG. 8b

FIG. 8.—(a) Same as Fig. 1, but for G339.88-1.26. Source 1 is clearly elongated at N; however, there may be another source seen at IHW18 just to the west. (b) A filled contour plot of source 1 at N with the 8.5 GHz radio continuum image of Ellingsen et al. (1996) overlaid. The radio continuum peak was assumed to be coincident with the mid-infrared peak. Methanol masers are shown as filled circles and are distributed at the same position angle as the mid-infrared elongation of source 1. The radio continuum seems to be extended perpendicularly to the mid-infrared source elongation and may be tracing an outflow. The OH masers of Caswell et al. (1995) are shown as open squares, and the water maser of Forster & Caswell (1989) is marked by the open circle. The size of the Gaussian restoring beam for the radio continuum is shown in the upper right of the plot.

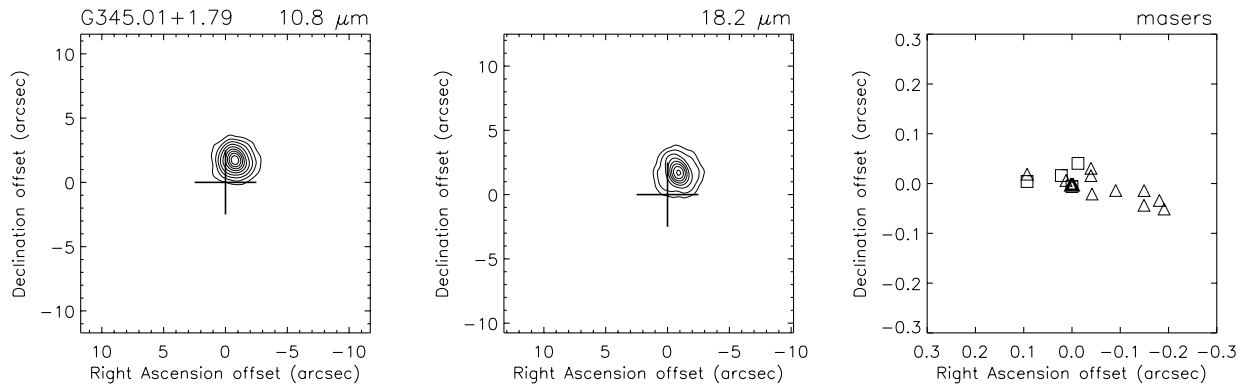


FIG. 9a

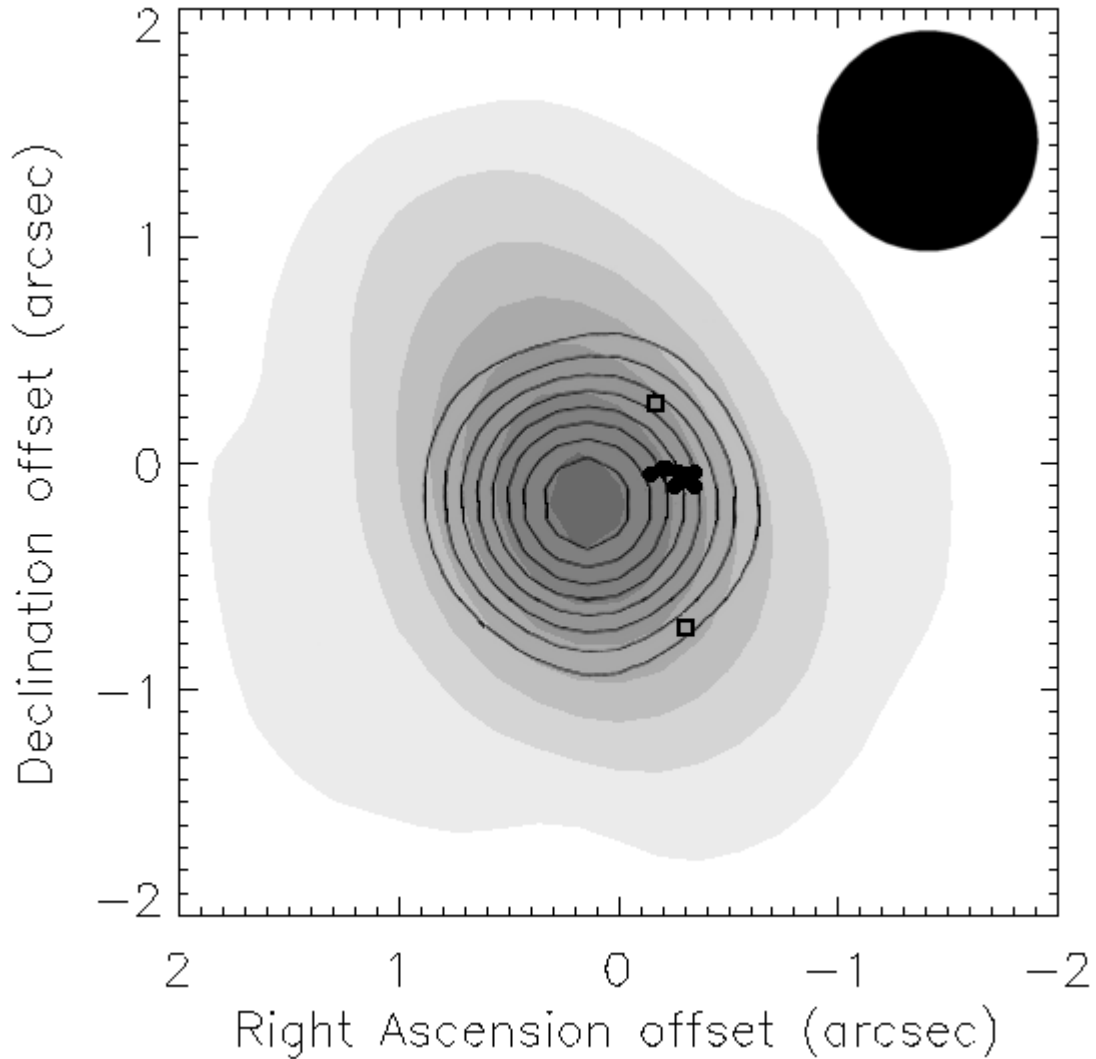


FIG. 9b

FIG. 9.—(a) Same as Fig. 1, but for G345.01+1.79. The source appears elongated at IHW18. However, the PSF for this source is elongated in the north-south direction, and therefore the source elongation may not be real. (b) A filled contour plot of the IHW18 image with the 8.6 GHz radio continuum image of Walsh et al. (1998) overlaid. The radio continuum peak was assumed to be coincident with the mid-infrared peak. Methanol masers are shown as filled circles and seem to be distributed radially to the radio continuum and perpendicularly to the mid-infrared elongation. If the elongation is real, the methanol masers may be tracing an outflow. The OH masers of Caswell et al. (1995) are shown as open squares. The size of the Gaussian restoring beam for the radio continuum is shown in the upper right of the plot.

a position angle close to that of the mid-infrared elongation. The PSF image taken at this location is elongated north-south, so we cannot be sure if the source is truly elongated. If the source elongation is real, this is a large discrepancy in position angle between the methanol maser distribution and mid-infrared elongation angle. Given the fact that these methanol masers are offset from the center of the UC H II region by  $0''.5$  and distributed radially, they may be tracing an outflow, as suggested by Walsh et al. (1998), and the OH masers may be coming from a disk in the perpendicular direction whose elongation we may be marginally resolving.

#### 4.14. G345.01 + 1.80

This site lies only  $19''$  away from G345.01 + 1.79. Caswell (1997) finds no UC H II region at 6 GHz, and neither does Phillips et al. (1998) with an upper limit on the peak 8.5 GHz continuum emission of  $0.7 \text{ mJy beam}^{-1}$ . Walsh et al. (1999) also failed to detect a source at this location in the near-infrared. Interestingly, this site has also been found to contain no OH maser emission. Caswell (1997) confirm the Norris et al. (1993) observations of the existence of a linear distribution of four methanol maser sources, spread over  $0''.22$  with three of the four spots showing a velocity gradient. The adopted distance to this region is the same as for G345.01 + 1.79.

We report here a discovery of a weak mid-infrared source at a low S/N at both  $N$  ( $0.2 \text{ Jy}$ ) and IHW18 ( $0.9 \text{ Jy}$ ). Because of the low S/N we cannot say anything about the morphology of the source other than it looks at this detection level to be point-like (Fig. 10).

#### 4.15. G351.42 + 0.64 (NGC 6334F and NGC 6334F – NW)

G351.42 + 0.64 is the location of a well-known cometary-shaped UC H II region named NGC 6334F (Rodriguez, Canto, & Moran 1982). The methanol masers are known to exist here in two sites separated by about  $6''$  (Norris et al. 1998).

The southern group of methanol masers is associated with NGC 6334F and are accompanied by OH masers, which run in a north-south line (Caswell 1997). Approximately  $4''$  north of the OH masers, water masers are known to exist in a linear pattern, pointing radially north away from the UC H II region peak (Carral et al. 1997). The distribution of methanol masers in NGC 6334F does not appear to be linear, but does have a similar velocity range to that of the OH masers ( $-13$  to  $-6 \text{ km}^{-1}$ ; Caswell 1997; Caswell et al. 1995), and does not display a systematic velocity gradient (Norris et al. 1993). Recombination lines

associated with the UC H II region yield a systemic velocity of  $-4 \text{ km}^{-1}$  (Forster et al. 1990).

Caswell (1997) find no 6 GHz radio continuum (same as Ellingsen et al. 1996) at the northern methanol maser site, NGC 6334F-NW. Also, NGC 6334F-NW does not have any associated OH or water masers. Again, there is no velocity gradient along the spots in the northern group.

Walsh et al. (1997) determined a distance to this site of either 1.9 or 12.9 kpc. This near distance is slightly different than the accepted value of 1.7 kpc, photometrically found by Neckel (1978). At the distance of 1.9 kpc, Walsh et al. (1997) determine this site would contain an O7 star with a luminosity of  $1.1 \times 10^5 L_{\odot}$ , if it contained one star.

Harvey & Gatley (1983) observed  $20 \mu\text{m}$  infrared sources at the locations of both NGC 6334F-NW (to within  $1''$ , named IRS2) and NGC 6334F (IRS1). We see at least four mid-infrared sources in this region (Fig. 11a). The UC H II region NGC 6334F is very prominent, and labeled source 1 in Figure 11. The infrared source associated with NGC 6334F-NW, our source 3, can best be seen at IHW18. Just to the east of the UC H II region is an elongated mid-infrared object, source 2.

Another source (or sources) is seen about  $14''$  east of the NGC 6334F, our source 4. This is designated IRS3 by Harvey & Gatley (1983). IRS3 appears to be a double source in the IHW18 images positioned in the north-south direction. It might also be an edge on circumstellar disk, as pointed out by Kraemer et al. (1999), who base this assumption upon morphology only.

We once more used the technique of registering our mid-infrared images with radio maps (as in § 4.3) to achieve better relative astrometry between the mid-infrared sources and maser positions. In this case we used the radio maps of Caswell (1997) and conclude that the southern methanol masers seem to be located at the sharp western boundary of the mid-infrared contours of the UC H II region (source 1, see Fig. 11b). These masers may therefore be associated with a shock front rather than a circumstellar disk. This astrometry also places the northerly group of methanol masers about  $1''.5$  below source 3. These masers may also be tracing an outflow or shock region rather than a disk.

This area is also the site of a large-scale CO outflow, with a lobe redshifted in the northeast direction and another blueshifted in the southwest direction. Some authors speculate that NGC 6334F-NW may have a disk and be the source of the outflow; however, our thermal images show this source to be resolved and elongated in the east-west direction, and the position angle of the source elongation is

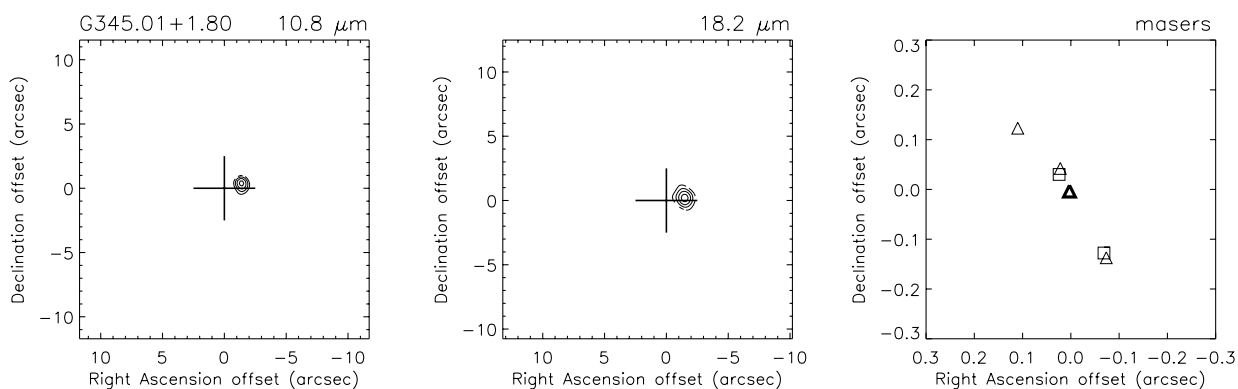


FIG. 10.— Same as Fig. 1, but for G345.01 + 1.80. The source is very low signal-to-noise.

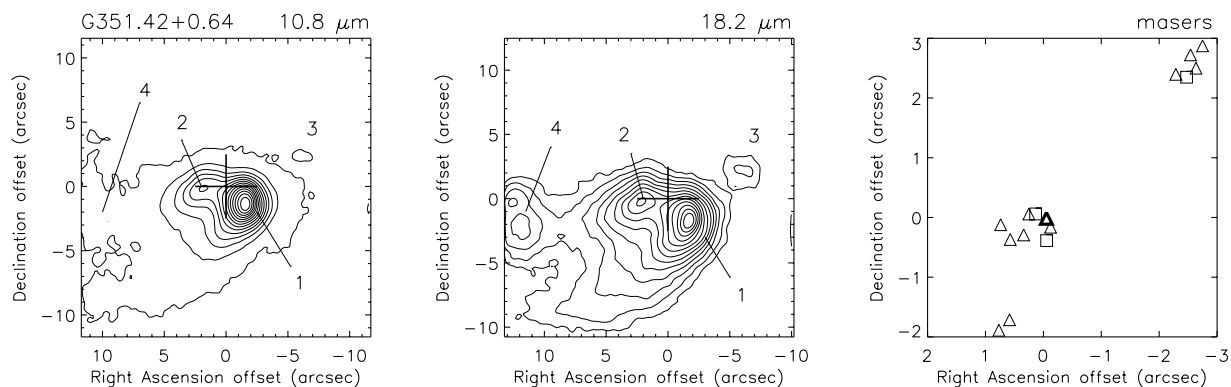


FIG. 11a

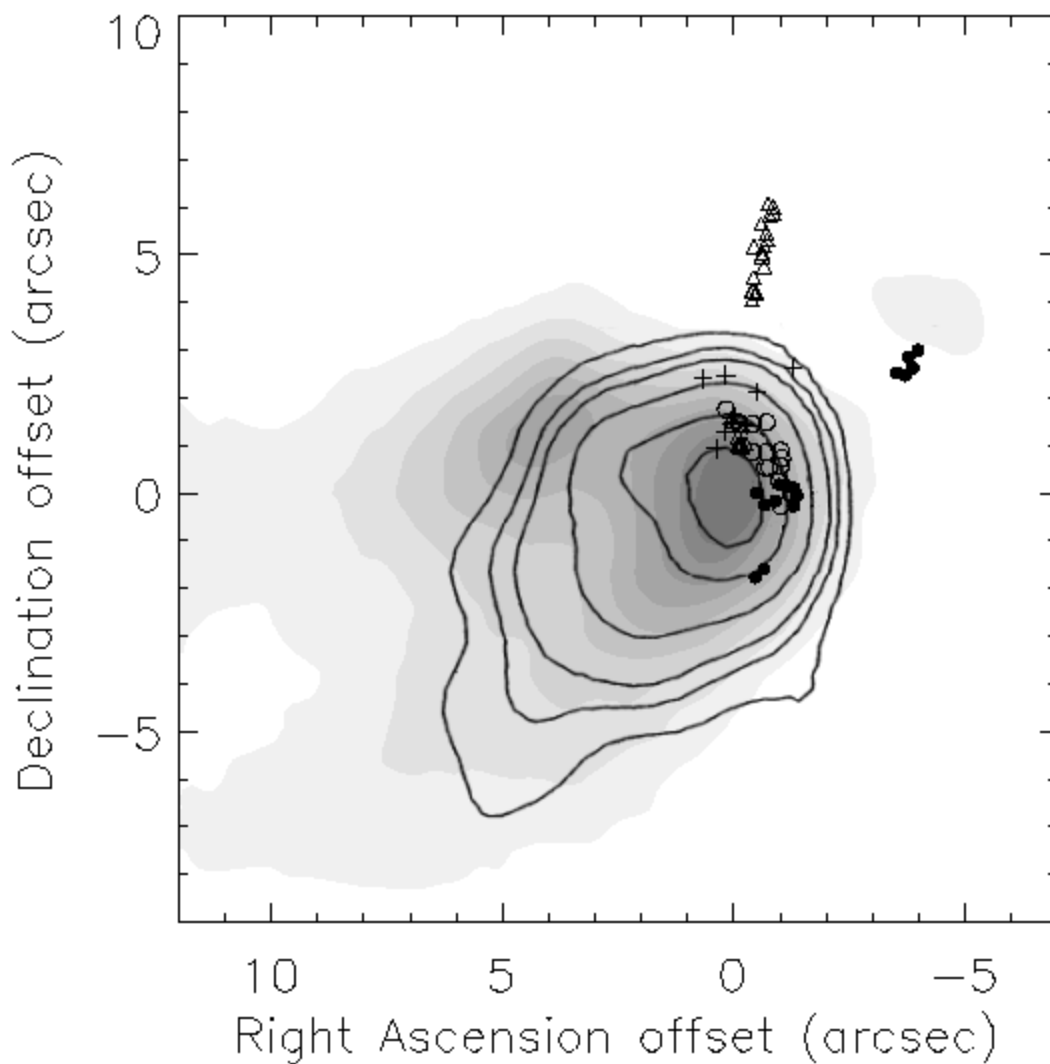


FIG. 11b

FIG. 11.—(a) Same as Fig. 1, but for G351.42+0.64. Our source 1 is coincident with the UC H II region NGC 6334F, which is also known as IRS1 (Harvey & Gatley 1983). Source 3 is known as NGC 6334F-NW, or IRS2. Source 4 is also known as IRS3. (b) A filled contour plot of the IHW18 image with the 6.7 GHz radio continuum image of Caswell (1997) overlaid. The radio continuum peak was assumed to be coincident with the mid-infrared peak. Methanol masers are shown as filled circles. The OH masers of Gaume & Mutel (1987) are shown as open circles, whereas the OH masers of Forster & Caswell (1989) are shown as crosses. The OH masers and methanol masers seem mixed both spatially and in velocity, and most likely trace the shock associated with the sharp western boundary of the expanding UC H II region. The methanol masers near source 3 are not coincident with the mid-infrared source and may be tracing an outflow. The water masers of Forster & Caswell (1989) are also plotted here as triangles and may be tracing an outflow from source 1 as well.

not parallel to that of the methanol maser distribution nor perpendicular to the outflow axis. Other authors speculate that NGC 6334F is the center of the outflow, but water masers are seen emanating to the northwest in a linear fashion and are thought to be tracing an outflow or jet (Fig. 11b). If this is the case, NGC 6334F would most likely not be the source of the outflow to the northeast as well. The elongated source 2 is near the center of the CO outflow and is perpendicular to the outflow axis. This could mean that source 2 may be a disk, and the outflow may originate there. Source 3 (NGC 6334F-NW) may be a disk, but the methanol masers may instead trace a southerly outflow since they are offset from the mid-infrared peak and distributed almost perpendicular to the mid-infrared elongation.

#### 4.16. *G351.44+0.66*

Although included in their survey, Norris et al. (1993) do not present any data on this source, and we did not detect any objects at this site in the mid-infrared. There is also a dearth of information in the literature on this particular site as well. We therefore do not consider this object any further in this paper.

#### 4.17. *G351.77-0.54*

This site contains the largest peak intensity of any known OH maser, at 1000 Jy (Caswell et al. 1995). It is also found to contain a highly variable OH and methanol maser (Fix et al. 1982; Caswell et al. 1995). Norris et al. (1993) only found four methanol masers here coincident with the location of these OH masers, and they display a well-defined velocity gradient along the spots. Forster & Caswell (1989) detected a water maser about 3" west of the OH and methanol maser location.

Walsh et al. (1997) found four methanol sources here, like Norris et al. (1993), but could not determine a useful distance to the site because of large errors associated with the observations of this location. However, Caswell (1997) determined the distance to be either 1.9 or 15.0 kpc and reason that the far distance is unlikely because the source is greater than 0.5 from the Galactic plane.

This is another site considered by Caswell (1997) to be a "steep-spectrum" *IRAS* point source. They derive the spectral type (using their distances above) for a single star based upon the FIR *IRAS* data to be B0.0, and from their radio work B0.3 for 6 cm or B0.4 for 20 cm emission.

Fix et al. (1982) observed this site at 5 and 1.4 GHz and find a large, amorphous continuum source (310 mJy at 5 GHz) lying almost 12" directly east of the OH maser loca-

tion. Haynes, Caswell, & Simons (1979) observed a very weak continuum source at the location of the OH masers at 5 GHz, which Fix et al. (1982) also see weakly (3 mJy) in the same location at 5 GHz but not at 1.4 GHz. Walsh et al. (1998) also detected the extended continuum associated with the UC H II region lying 12" to the east of the OH masers at 8.6 GHz. However, they find nothing at the maser location. Hughes & MacLeod (1993) believe that they have discovered a binary source associated with the location of the OH and methanol masers at a resolution of 0.3 at 6 cm. They also see the diffuse continuum source 12" to the east. They believe that this diffuse source contains about 12 B0.5 stars.

Fix et al. (1982) and Walsh et al. (1999) also observed *K*-band sources at both sites. Fix et al. (1982) claims the near infrared object at the location of the masers is extended (15"–20" in diameter) and has uniform surface brightness ( $K = 10.7$ ). However, images by Walsh et al. (1999) show that these may be several field stars, but they do find a single source coincident with the methanol masers at *L* and a source coincident with the extended radio emission to the east. Fix et al. (1982) looked for, but did not detect any 10  $\mu$ m sources, but they did find evidence for extended CO emission in the area.

Caswell (1997) points out that the velocity spreads in all the maser types are large. The water masers at this site observed by Forster (1990) covered a velocity range of  $-38$  to  $+22$  km  $^{-1}$ . They are also arranged in a circular fashion over an area on 4". Some are found to be blueshifted and others redshifted, and the overall geometry is similar to that of an expanding ring. They conclude that the compact size, wide velocity spread in the masers, and a lack of strong continuum emission points to this being a star in its early expansion phase (Forster & Caswell 1989). They also point out that the geometry may be due to outflow of some kind.

We detected a compact, low S/N object at a location about 10" east of the position of the methanol masers (Fig. 12, source 1). We further detected a very diffuse and large extended object (source 2) about 3" northeast of the maser location. At such a low detection level it is difficult to comment much on the morphologies or coincidences of these sources.

#### 4.18. *G9.621+0.196 and G9.619+0.193*

This region contains two methanol maser sites separated by  $\sim 12''$  in declination. The northern site, *G9.621+0.196*, contains a 6.7 GHz methanol maser with the highest flux known. Norris et al. (1993) observed methanol masers at

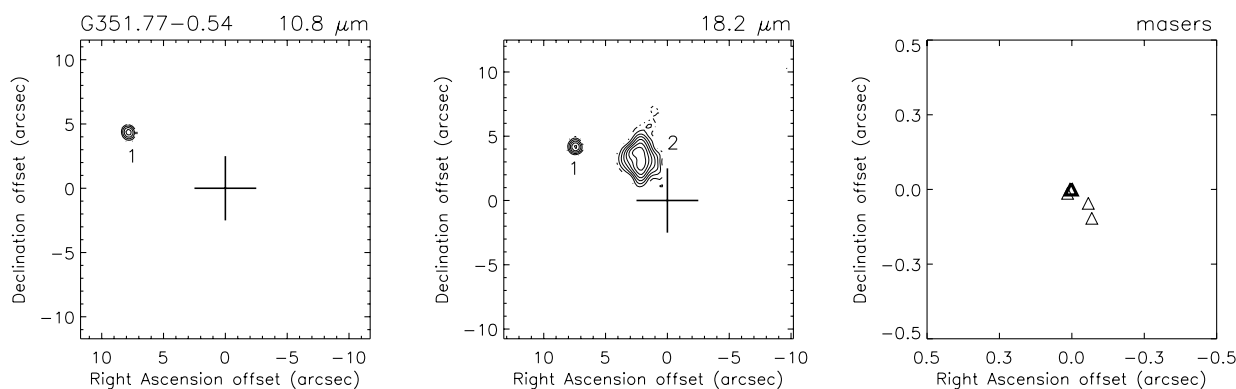


FIG. 12.— Same as Fig. 1, but for *G351.77-0.54*. It is not known if source 2 is real. Both sources are low signal-to-noise detections.

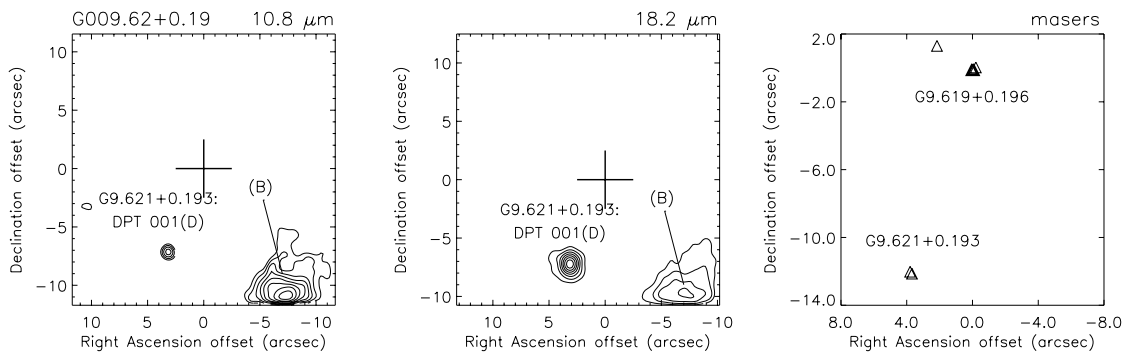


FIG. 13a

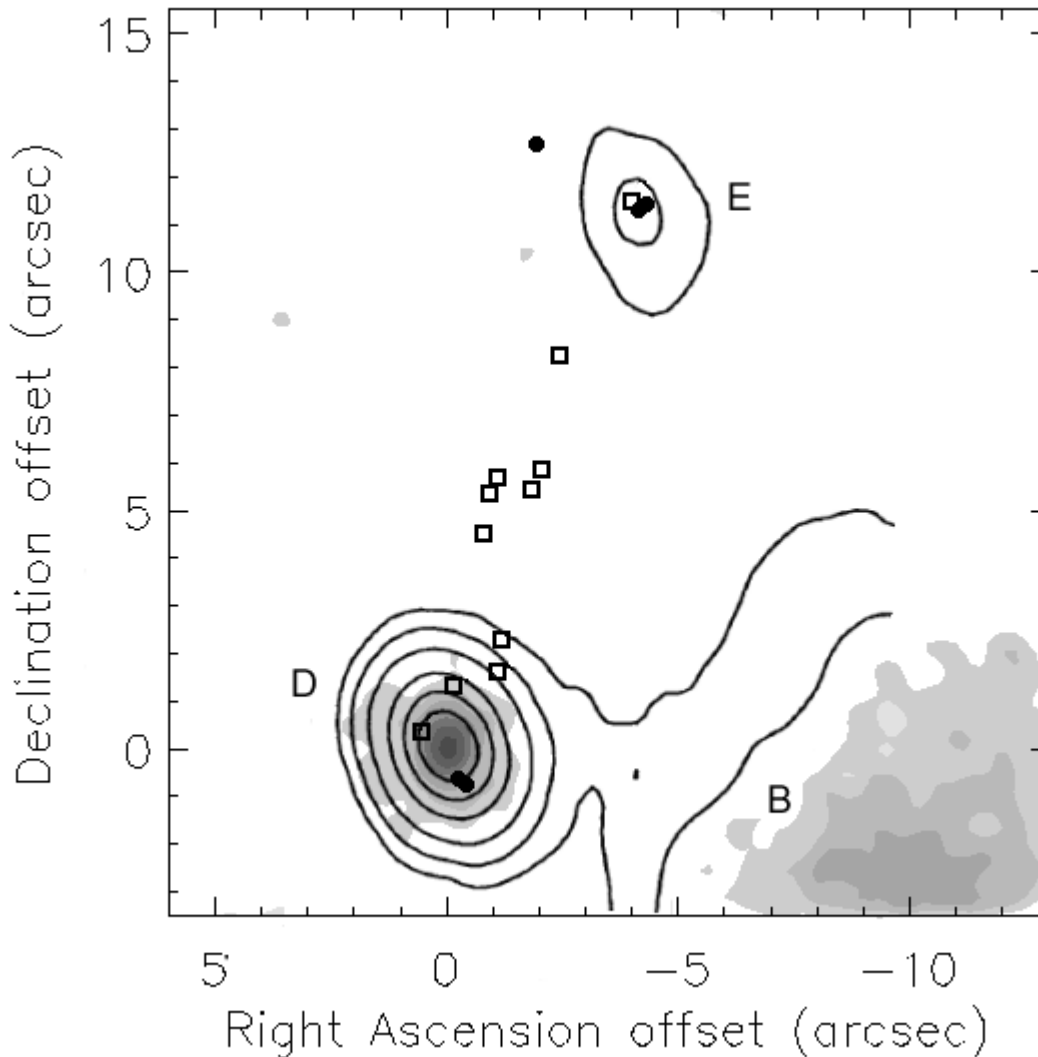


FIG. 13b

FIG. 13.—(a) Same as Fig. 1, but for G9.62+0.19. This site contains both maser sources G9.621+0.196 and G9.619+0.193. We detected a mid-infrared source associated with G9.619+0.193 only. Labels in parentheses are sources from Garay et al. (1993). (b) A filled contour plot of the IHW18 image with the 23 GHz radio continuum image of Cesaroni et al. (1994) overlaid. The radio continuum peak was assumed to be coincident with the mid-infrared peak. The radio continuum sources B, D, and E (using the nomenclature of Garay et al. 1993) are indicated. Methanol masers are shown as filled circles. The water masers of Hofner & Churchwell (1996) are shown as open squares, and form a line stretching from radio components D to E.

both sites and consider them to be compact or complex, with no linearly distributed methanol masers. Forster & Caswell (1989) also found OH masers coincident with the two groups of methanol masers.

Norris et al. (1993) observed three masers at the location of G9.621+0.196. It was also found to contain a 19 mJy source at 15 GHz by Garay et al. (1993), which they call source E. Nothing was detected in the 8.6 GHz maps (3.5

cm) of Walsh et al. (1998), or the 3.6 cm continuum map from the VLA by Kurtz, Churchwell, & Wood (1994). However, Cesaroni et al. (1994) and Hofner & Churchwell (1996) did observe a source at the location of G9.621+0.196 at 1.3 cm. Not only is this source coincident with a thermal ammonia core, but among the methanol masers is located the first ever discovered  $\text{NH}_3(5,5)$  maser (Cesaroni et al. 1994).

The southern site, G9.619+0.193, was found to contain two 6.7 GHz methanol masers by Norris et al. (1993). It also contains a 110 mJy source observed at 15 GHz by Garay et al. (1993), which was named source D. Walsh et al. (1998) find a single unresolved 8.6 GHz (3.5 cm) continuum source in this location coincident with two methanol masers, whereas Kurtz et al. (1994) did not. Hofner & Churchwell (1996) and Cesaroni et al. (1994) find 1.3 cm radio emission at this location, as well. Walsh et al. (1998) point out that the G9.619+0.193 methanol masers associated with the D source are offset about  $1''$  to the south of the peak in the radio continuum emission.

This site also contains a large ( $\sim 15''$ ), diffuse and amorphous H II region located west and south of G9.619+0.193 by about  $14''$  (Walsh et al. 1998; Hofner & Churchwell 1996; Kurtz, Churchwell, & Wood 1994). Cesaroni et al. 1994 detect the 1.3 cm continuum of this large HII region. Garay et al. (1993) detect this site at 15 GHz and call it source B. Continuum maps at 2 and 3.6 cm at the VLA by Kurtz et al. (1994) show the source as well.

Interestingly, there is a string of water masers found by Hofner & Churchwell (1996) extending from the location of the methanol masers at G9.621+0.196 to the methanol masers at G9.619+0.193. Also, found lying stretched between the two locations is thermal ammonia emission (Hofner et al. 1994).

Cesaroni et al. 1994 detect an additional continuum source further north of G9.621+0.196. To use the nomenclature of Garay et al. (1993), the source furthest to the north is the C source. Continuum maps at 2.0 and 3.6 cm at the VLA by Kurtz et al. (1994) show C. Another source, source A of Garay et al. (1993), is further west of the H II region B, and is another large ( $30''$ ) and diffuse HII region.

There is considerable disagreement about the distance to this site. Wink, Altenhoff, & Mezger (1982) derived distances of 0.6 and 19.1 kpc, and consider the near distance most likely based on the absence of  $\text{H}_2\text{CO}$  absorption. Garay et al. (1993) feel that the source lies at a far distance of 16.1 kpc, based on the observed UV-to-radio luminosity ratio. Kurtz et al. (1994) obtained near and far distances of 0.7 and 16.1 kpc, consistent with the distance of Wink et al. (1982). Walsh et al. (1997) could not determine a distance to this site because of large errors. A distance of 0.6 kpc seems to be the best distance because it is based on absorption-line measurements.

This seems to be a very complex site which appears to be a ridge of molecular material, as evidenced by the string of water masers and elongated distribution of thermal ammonia, where star-forming activity is present in at least three centers. Our mid-infrared observations reveal the large diffuse H II region (source B of Garay et al. 1993; see Fig. 13), as well as an unresolved mid-infrared source at the location of the southern maser location G9.619+0.193. Interestingly, Walsh et al. (1999) found no evidence of a near-infrared source at this location. Like Walsh et al. (1999), we see no signs of a thermal infrared source at the

site of the northern masers of G9.621+0.196, nor the most northern radio source C (source A was not in our field).

## 5. DISCUSSION

### 5.1. *Summary of Mid-Infrared Sources Associated with Linearly Distributed Methanol Masers and the Circumstellar Disk Candidates*

In our mid-infrared survey of 21 sites, 10 have methanol masers distributed linearly. Of those 10, we detected mid-infrared sources in 8. Three of those eight sites have sources that are resolved at mid-infrared wavelengths by our survey. All three resolved sources are elongated at the same position angle as their associated methanol masers. These sources are G309.92+0.48:DPT00 1, G323.740-0.263:DPT00 1, and G339.88-1.26:DPT00 1, all of which appear the most elongated at  $18 \mu\text{m}$ . Interestingly, the three resolved sources are in close proximity to other sources which lie at similar position angles to the maser distribution angles.

Of the remaining five mid-infrared source detections where the methanol masers are linearly distributed, there appears to be an elongated source associated with G328.81+0.63:DPT00 2, which is in a close pair of sources. By subtracting out a Gaussian model for source 1, we were able to remove the source, leaving an elongated source 2. This may be another case where one source in a double is elongated at the same position angle as the methanol maser distribution. However, higher resolution images are needed to resolve both sources and see if source 2 is truly elongated.

The two sources, G318.95-0.20:DPT00 1 and G331.28-0.19:DPT00 1 appear slightly elongated at the position angle of the methanol masers. The FWHM major-to-minor axis ratio for both of these is 1.3. However, the PSF stars for these objects are elongated in the same direction and with the same axis ratio. Therefore, we consider these sources to be unresolved.

The two remaining mid-infrared detections showing linearly distributed methanol masers are G345.01+1.79 and G345.01+1.80. In the case of G345.01+1.80:DPT00 1, we barely detect a source at 10 and  $18 \mu\text{m}$ . With such low S/N, we cannot comment on its morphology. G345.01+1.79 is an elongated source whose mid-infrared position angle is different from the methanol maser position angle. However, we again point out that this object is marginally resolved at best, and the PSF observations nearby are elongated in the north-south direction. If the elongation is real, these masers may be associated with a different process such as outflow.

Also resolved were the sources associated with the methanol masers of NGC 6334F, NGC 6334F-NW, and G328.25-0.53. Both NGC 6334F and NGC 6334F-NW are considered to have linear distributions of methanol masers by Norris et al. (1993). However, the masers of NGC 6334F are spread out over a relatively large area of  $1 \text{ arcsec}^2$ . We do not consider these masers to be linearly distributed, and when viewed with the other masers in the area (Fig. 11b), the methanol masers seem to follow the OH masers in tracing the contours of the sharp edge of the UC H II region. We believe these methanol masers exist in the shock front of the UC H II region of NGC 6334F. As for the resolved source associated with NGC 6334F-NW, we see that the mid-infrared source is offset from the methanol masers by  $\sim 1''.5$ . These masers may exist in an outflow, rather than tracing a disk, or may be associated with a

deeply embedded source just south of NGC 6334F-NW. For G328.25–0.53, we are not sure where exactly the masers are located with respect to our mid-infrared sources; however, we are certain they are most closely associated with our source 2. This source is elongated at a similar position angle to the western group of three methanol masers. However, there are other masers nearby (Norris et al. 1993 describe this maser site as complex), and given our astrometry we cannot ascertain which masers are coincident with our source 2.

As mentioned earlier, the resolved sources G309.92+0.48:DPT00 1, G323.740–0.263:DPT00 1, and G339.88–1.26:DPT00 1 exist near other sources which lie at similar position angles to the maser distribution angles. However, at separations of 24000, 12000, and 9000 AU, respectively, it seems unlikely that these are gravitationally bound binaries. Nevertheless, wide binaries could initially form via the growth of an instability in the outer parts of a massive circumstellar disk (Bonnell 1994). In this formation scenario, the spin axes of the binary components will always be aligned, and their circumstellar disks would be coplanar to the binary position angle. Observational evidence seems to support the hypothesis that wide binaries form in such a way to produce coplanarity. Polarimetry work by Monin, Menard, & Duchene (1998) of binaries with separations between 1200 and 5200 AU show that the binary components have preferentially the same orientations. Even at smaller separations (200–1000 AU), polarimetry of disks around binary components have been observed to be preferentially aligned with each other (Jensen et al. 2000).

Norris et al. (1993) argue that the simplest explanation for the observed properties of the linearly distributed methanol masers is that they lie in circumstellar disks. While it seems not all linearly distributed masers trace disks, there does seem to be much circumstantial evidence that points to this being the case for our circumstellar disk candidates. Three of the eight thermal sources we observed are coincident with, and elongated at the same position angle as the methanol masers. In all three cases the methanol masers overlap the radio continuum and mid-infrared peaks to within an arcsecond. This means that the masers are most likely coincident with the stellar/protostellar source, which is a requirement if they trace disks. In the case of G309.92+0.48:DPT00 1, the methanol masers have a well defined velocity gradient indicative of some sort of rotation. Furthermore, all three disk candidates have sources nearby that lie at similar position angles as the methanol maser distributions, and observational evidence points to binary formation mechanisms which favor binary components with disks aligned to the same position angle as the binary system. It seems the simplest explanation for the thermal elongations of G309.92+0.48:DPT00 1, G323.740–0.263:DPT00 1, and G339.88–1.26:DPT00 1 is that they are indeed circumstellar disks.

### 5.2. The Nature of Massive Stars Exhibiting Methanol Maser Emission

Of the 21 sites of methanol maser emission in our survey, Phillips et al. (1998) finds only 11 have detectable radio continuum. The absence of UC H II regions has also been observed by Walsh et al. (1998) to be a general characteristic of methanol maser sites. Likewise, Caswell (1996) finds that only three out of 57 sites contain UC H II regions in a methanol maser survey. There are several reasons suggested

as to why many methanol maser sites lack detectable UC H II regions (outlined by Phillips et al. 1998), but three seem to be most viable: (1) The stars associated with the maser emission may be at the earliest stages of stellar formation, and are deeply embedded. Therefore, they would have little or no detectable radio continuum emission because infall from the surrounding envelope would confine the UC H II region to the immediate vicinity of a star, making the surroundings optically thick in the radio and keeping the ionized region geometrically small in projected area. Tofani et al. (1995) observe a lower frequency of association of H<sub>2</sub>O masers with UC H II regions and use this hypothesis to explain their data. (2) The stars associated with the maser emission may be less massive stars that are nonionizing or weakly ionizing. According to Churchwell (1991), stars with spectral types later than B3 do not produce enough Lyman-alpha continuum photons to effectively produce a detectable UC H II region at the kiloparsec distances of the massive stars such as those in our survey. (3) The methanol masers are not associated with a process directly coincident with a forming star. For instance, a star with an outflow impinging on knots of interstellar material in the vicinity of the star could produce a shock front that would collisionally excite maser emission.

Walsh et al. (1998) favor explanation (1). They propose that methanol maser emission begins at the earliest stages of star formation, before the stars are hot enough or evolved enough to ionize their surrounding gas, and continues for 40% the lifetime of the UC H II region and then shuts off. However, given the near-infrared data of Walsh et al. (1999), this seems to be an unlikely scenario. Of the nine sites of methanol maser emission without UC H II regions in our survey, four are seen in the survey of Walsh et al. (1999) at *K* (three of these have been seen at *H* as well). If these four sources are at such an early stage of formation that they are not producing significant UC H II regions, they would be so highly embedded that there should be no detectable emission at near-infrared wavelengths. Instead, because these sources can be seen in the near-infrared and do not have any detectable radio continuum emission, it seems most likely that they are young, but less massive stars of weakly ionizing spectral types. Consistent with this idea, our lower limits to the bolometric luminosity from our mid-infrared fluxes given in Table 3 yield a range in spectral types between B6.9 and A3.7 (excluding G305.20+0.21:DPT00 1) for sources without UC H II regions, and a range of B0.7–B6.8 (excluding G9.619+0.193:DPT00 1) for sources with UC H II regions<sup>2</sup>. Furthermore, of the seven mid-infrared sources that do not have radio continuum emission (Table

<sup>2</sup> We have excluded G305.20+0.21:DPT00 1 and G9.619+0.193:DPT00 1 from this discussion for the following reasons. G305.20+0.21:DPT00 1 is unique in that it has a flux at 11  $\mu$ m, which is twice as high as the *IRAS* flux for the region. It also has the highest flux at 18  $\mu$ m compared to its *IRAS* value (Table 3). Our lower limit estimate of the bolometric luminosity is greater than 12000  $L_{\odot}$  for this source. However, even though it is visible at all near and mid-infrared wavelengths and therefore cannot be heavily embedded, it has no radio continuum. Similarly peculiar is G9.619+0.193:DPT00 1, which has the largest differential in radio continuum derived spectral type compared to mid-infrared derived spectral type. The source was not detected at *L* by Walsh et al. (1999), and is brighter in our 18  $\mu$ m image, compared to the 10  $\mu$ m image. It may be that the mid-infrared flux is substantially reduced by foreground extinction, possibly associated with the nearby large H II region. If this is the case, it would result in a large underestimate of the true source luminosity.

3), six are either compact and unresolved, or have low S/N (or both). One would expect that lower mass stars would not heat dust as far out as the massive, ionizing stars, and it would therefore be harder to detect any extension in emission in the mid-infrared at the distances of these sources. This seems to imply that scenario (2) is most likely correct, and that the stars without UC H II regions are less massive and therefore do not produce detectable amounts of radio emission.

Table 3 also lists the four sources which display radio continuum, but do not have mid-infrared emission. These sources may be massive stars in an early stage of formation when they are too embedded to have detectable emission at near- and mid-infrared wavelengths and have not developed a sufficiently extended circumstellar ionized envelope. This would be analogous to the Class 0 phase of stellar evolution (Andre, Ward-Thompson, & Barsony 1993; Lada 1987), when the source is visible only at far-infrared wavelengths or longer.

The fourth section of Table 3 lists the two sites that have no near-infrared, mid-infrared, or radio continuum emission. There are two possible explanations for these two sites that only display methanol maser emission. First, these may be extremely young stellar sources that are so highly embedded that they are self absorbed at near- and mid-infrared wavelengths as well as being optically thick at radio wavelengths, as in scenario (1) above. The other possibility is that these sources of methanol maser emission are offset from a nonionizing star and are collisionally excited in an outflow. In this scenario, a young stellar source (of any mass) that is in outflow may have methanol maser emission associated with the shock of the outflow on the surrounding ambient gas or upon some nearby knot of material. Bachiller et al. (1998) observed spectacular enhancements of meth-

anol abundance toward the shocked molecular gas in the bipolar outflow of the low-mass young stellar source NGC 1333: IRAS 2. These areas of enhanced methanol abundance lie approximately 25,000 AU away from the stellar source. It is therefore plausible that methanol masers may form in these outflow shock zones, and this could very well be a scenario by which a significant portion of the methanol masers are generated.

### 5.3. The Relationships between Mid-Infrared, IRAS and Radio Observations

The closest *IRAS* sources associated with the methanol maser sites were determined from the *IRAS* Point Source Catalog. Table 4 shows the associated 12 and 25  $\mu\text{m}$  *IRAS* fluxes and the fluxes obtained at 10.46 and 18.06  $\mu\text{m}$  by our instrument for the whole area in our field of view. It should be pointed out that the offsets of the presumed center of the *IRAS* beam are anywhere from 4" to 2.5' from the actual location of the methanol maser location. We also found *IRAS* LRS (Low-Resolution Spectrometer) spectra (7 to 25  $\mu\text{m}$  wavelength range) for six of the sources in our survey (*IRAS* Science Team 1986; Volk et al. 1991; Chan, Henning, & Schreyer 1996). The monochromatic flux densities obtained from the LRS spectra at 11 and 18  $\mu\text{m}$  are also listed in Table 4, however we caution that objects less than 6' apart are considered to be confused.

Comparing the different flux densities observed for the sources in Table 4 shows that the *IRAS* PSC fluxes from the region associated with the methanol emission are, in many cases, much larger than the fluxes determined with our instrument. Because of its  $\sim 75'' \times 1.5'$  spatial resolution at 12 and 25  $\mu\text{m}$ , *IRAS* presumably measured flux from sources that lie outside our field of view, as well as extended emission associated with these sources. In many cases our

TABLE 4  
TOTAL INTEGRATED FLUX DENSITY OBSERVED IN THE OSCIR FIELD OF VIEW AND CORRESPONDING *IRAS*  
FLUX DENSITY MEASUREMENTS

Target Field	OSCIR N/IHW18 (Jy)	<i>IRAS</i> PSC Name	<i>IRAS</i> 12/25 $\mu\text{m}$ (Jy)	<i>IRAS</i> 11/18 $\mu\text{m}^a$ (Jy)	LRS 11/18 $\mu\text{m}^b$ (Jy)
G305.2+0.2 <sup>c</sup>	36.13/117.72	13079–6218	28.32/249.72	18.44/155.03	72/600 <sup>d</sup>
G309.92+0.48	50.25/208.60	13471–6120	76.31/667.88	49.76/415.67	...
G318.95–0.20	5.07/18.81	14567–5846	33.80/300.79	21.96/186.14	9/128 <sup>e</sup>
G323.74–0.26 <sup>f</sup>	1.17/8.81	15278–5620	23.57/166.66	16.41/110.38	33/80 <sup>g*</sup>
G328.2–0.5 <sup>h</sup>	1.12/3.94	15541–5349	12.04/110.69	7.52/68.18	...
G328.81+0.63	6.70/58.89	15520–5234	15.49/537.93	5.23/206.50	...
G331.28–0.19	1.02/3.27	16076–5134	35.96/237.28	24.42/160.86	35/217 <sup>d</sup>
G336.43–0.26	<0.01/<0.18	16306–4758	15.60/68.03	12.37/51.78	...
G339.88–1.26	0.99/15.15	16484–4603	9.93/192.04	4.76/92.08	...
G340.78–0.10	<0.02/<0.17	16465–4437	4.12/4.45	4.07/4.75	...
G345.0+1.8 <sup>i</sup>	6.01/28.39	16533–4009	26.40/471.28	12.88/232.26	25/405 <sup>d</sup>
G351.4+0.6 <sup>j</sup>	75.59/336.43	17175–3544	103.51/1400.36	56.77/758.54	...
G351.77–0.54	0.21/4.26	17233–3606	4.50/228.80	1.30/76.05	...
G9.62+0.19 <sup>k</sup>	0.25/3.59	18032–2032	38.63/292.41	26.00/191.14	38/133 <sup>e</sup>

<sup>a</sup> The color-corrected *IRAS* flux densities at 12 and 25  $\mu\text{m}$  were fit with a blackbody curve from which an extrapolated value was found at 11  $\mu\text{m}$  and an interpolated value was found at 18  $\mu\text{m}$ .

<sup>b</sup> Monochromatic flux density from *IRAS* low-resolution spectra.

<sup>c</sup> Combined fields of G305.20+0.21 and G305.21+0.21.

<sup>d</sup> From Volk et al. 1991.

<sup>e</sup> From *IRAS* Science Team 1986.

<sup>f</sup> Combined fields of G323.740–0.263 and G323.741–0.263.

<sup>g</sup> From Chan et al. 1996.

<sup>h</sup> Combined fields of G328.24–0.55 and G328.25–0.53.

<sup>i</sup> Combined fields of G345.01+1.79 and G345.01+1.80.

<sup>j</sup> Combined fields of G351.42+0.64(NGC 6334F and NGC 6334F–NW) and G351.44+0.66.

<sup>k</sup> Combined fields of G9.621+0.196 and G9.619+0.193.

observations reveal multiple sources that would be confused in the *IRAS* beam. It is therefore entirely reasonable that *IRAS* with its larger beam will likely detect more flux than we have detected with our instrument. Consequently, the single source associated with the methanol masers cannot be modeled correctly with the fluxes that were obtained by *IRAS* for the whole region surrounding the source. For instance, in § 4 we presented luminosities and spectral types for several sites from Walsh et al. (1997) and Caswell (1997), who both used *IRAS* far-infrared fluxes to derive their results. These should be considered in most cases to be extreme upper limits. In fact, spectral type estimates given by these authors are mostly O types. Interestingly, spectral types estimated from radio continuum and mid-infrared fluxes (Table 2) show that none of the stellar sources associated with methanol masers in this survey are as massive as an O star.

The LRS monochromatic flux densities we have tabulated are also larger than those determined with OSCIR. Given the 6' resolution, and the fact that O and B stars are often found in associations and complexes, flux values for these maser sources are most likely not well determined by the LRS spectra either. Furthermore, a simple interpretation of the LRS silicate features for the sources associated with the methanol masers is not possible. Comparisons of our data to the LRS monochromatic fluxes support these assumptions, by virtue of the LRS flux density values being 2 to 58 times larger than the OSCIR values. Likewise, we described in § 4 several sources which are considered "steep spectrum" or contain a "21  $\mu\text{m}$  feature," as determined from the LRS spectra. Once again, it is hard to determine the significance of these spectral features as they relate only to the stellar sources associated with the maser emission.

It has been suggested that methanol masers may be pumped by far-infrared radiation. Interestingly, van der Walt, Gaylard, & MacLeod (1995) and Walsh et al. (1997) show that there is little to no correlation between the methanol maser flux densities observed and *IRAS* flux densities, which seemingly contradicts this hypothesis. Furthermore, since the methanol masers are directly coincident with young stellar sources, far-infrared pumping seems unlikely because the far-infrared emission from cool material might exist too far from the maser sources to be the dominant pump mechanism. Walsh et al. (1997) point out that some methanol masers exist where there is no apparent far-infrared radiation and state that methanol masers seems more dependent on the abundance of methanol instead.

In addition to the lack of correlation with far-infrared radiation, Walsh et al. (1998) could not establish any correlation between radio continuum emission and methanol maser emission. Indeed, many sites of methanol maser emission have no detectable radio continuum emission. This therefore seems to show that maser emission cannot be significantly influenced by radio continuum photons.

Data from this survey were compared to several methanol maser parameters as well, to see if there were any trends or correlations. There seems to be no relationship between mid-infrared flux and methanol maser flux (i.e., peak spot flux, average spot flux, or summed flux for all spots), nor between mid-infrared flux and number of maser spots.

Extensive modeling has been performed for the 6 and 12 GHz maser transitions by Sobolev & Deguchi (1994) and Sobolev, Cragg, & Godfrey (1997). They conclude that the

methanol masers lie in projection against the background of radio continuum photons from a UC H II region, which provides the source photons for amplification. Pumping is achieved not by far-infrared photons, but through mid-infrared photons emitted by the warm greater than 150 K dust that surrounds the methanol-rich matter near the YSO. These mid-infrared photons provide an infrared continuum source close enough to the location of the maser to pump the methanol to the first and second torsionally excited states required for the maser transition.

Consistent with this modeling, we find a possible relationship between mid-infrared source size and methanol maser distribution in our survey. Figure 14 shows 18  $\mu\text{m}$  infrared source sizes versus extent of the maser spot distribution. Here we plot only the mid-infrared sources that we could directly identify as being coincident with the methanol masers, and hence may be radiatively rather than collisionally pumped. The plotted infrared source sizes are from the longest axis of the mid-infrared source, and had PSF FWHM subtracted in quadrature. Also plotted is the 1:1 line. Figure 14 suggests a trend in which larger methanol maser distributions correspond to larger mid-infrared emitting regions. But more importantly, all of the points in the plot lie above the 1:1 line, indicating that conditions for methanol maser emission lie within the mid-infrared emitting regions, if we assume that the methanol masers are

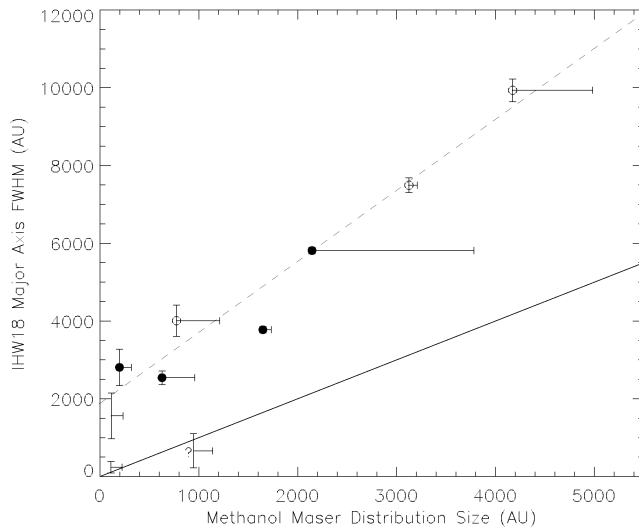


FIG. 14.—Methanol maser distribution size vs. physical *IHW18* extent for all sources where masers are coincident with the mid-infrared sources. Open circles represent the FWHM of the disk candidates along the axis parallel to the methanol maser distribution. Left to right, these are G232.740–0.263, G339.88–1.26, and G309.92+0.48. The filled circles (left to right) represent resolved sources G328.25–0.53, G345.01+1.79 (which may be marginally resolved), NGC 6334F (which has methanol masers that may instead be located in shock regions), and G328.81+0.63. The *IHW18* PSF was subtracted in quadrature from each FWHM. The sources plotted without symbols are unresolved, and the error bars in the *y*-direction show the range between the resolution limiting upper-limit and blackbody lower-limit size. Top to bottom these are G305.20+0.21, G318.95–0.20, and G9.621+0.196. Errors in the *x*-direction for all points are taken to be the average separation between maser spots. The solid line is the line indicating when the *IHW18* size is equal to the methanol maser distribution extent. Notice that all of the points plotted lie above this line, indicating that the masers preferentially lie within the mid-infrared emitting region (except for G318.95–0.20, marked with a question mark, whose masers are offset by 2.5 and may not be associated with the mid-infrared source). The dashed line is a least squares fit to the points. There seems to be a rough correlation between mid-infrared size and methanol masers distribution size.

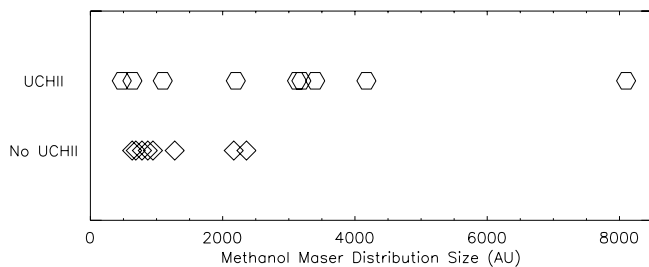


FIG. 15.—Methanol maser distribution sizes for sources with UC H II regions (hexagons) and without UC H II regions (diamonds). The sources with UC H II regions have methanol masers spread over a larger region, than those without UC H II regions. Furthermore, this plot shows most sources lacking UC H II regions have their methanol maser distributed over less than 1000 AU.

coincident with the mid-infrared peaks. This is the first direct observational evidence that the mid-infrared flux associated with the warm, dense, molecular gas and dust is the main contributor to the pumping of methanol masers.

Figure 15 shows the extent of the maser spot distribution for the population of sources in our survey with UC H II regions and for the population without UC H II regions. The sources with UC H II regions tend to have methanol masers distributed over a larger physical extent, than those without UC H II regions. A majority of sources without UC H II regions have methanol maser distributions spanning less than 1000 AU. This supports the hypotheses advanced here that methanol masers are contained within the mid-infrared emitting region. If the hypotheses that methanol masers are pumped by mid-infrared photons is correct, one would expect to see methanol masers come from the larger extents for the sources with UC H II regions. This is because our analysis has shown that stars without radio continuum are most likely less massive stars. The higher mass ionizing stars would produce a flux capable of heating out to larger distances than lower mass nonionizing stars. Therefore, not only would the methanol maser distribution extents be smaller, but so would the mid-infrared sources. We see in Table 3 that all of the sources without UC H II regions (except for G323.740–0.263), are unresolved or have low signal-to-noise (or both).

The modeling described above and our subsequent observations may explain methanol maser excitation and pumping in the presence of a UC H II region, but it does not easily explain the presence of methanol masers where there are no UC H II regions and no apparent mid-infrared flux. If these objects are less massive stars, we would expect there would be little radio continuum to amplify. However, it is pointed out by Sobolev et al. (1997) that for sources with no UC H II regions, one could get high enough maser brightness temperatures at 6.7 GHz from the amplification of 2.7 K microwave background photons alone. Pumping would still need to be achieved via a warm, methanol rich dust clump, or perhaps several clumps in a disk.

#### 5.4. Alternatives to the Disk Hypothesis

Recent papers have suggested that linearly distributed methanol masers can best be described by a shock model. Sobolev & Deguchi (1994) and Walsh et al. (1998) both advance a shock hypothesis, but each with a variation on that central theme.

Sobolev & Deguchi (1994) and Sobolev et al. (1997) describe a “clump” hypothesis in which the maser sources

are separate elongated clumps of material. They suggest that a shock front, preceding the ionization front delimiting the UC H II region of a forming star, impinging on the surrounding interstellar cloud could create the clumps, or the clumps could be preexisting, interstellar knots of material. Conditions for the existence of methanol masers in these clumps, such as methanol abundance, density enhancement, and radially elongated structures, are argued to be produced by the shock wave itself. The portion of the shock wave moving towards the observer would create the necessary geometry and conditions for the masers because the radially elongated masing clumps would be projected in front of a background of radio continuum emission. They further point out that the shock could also align the clumps, and in the process possibly distribute them in some organized fashion. A problem with this scenario is that the gas temperature behind shocks are high (Frail & Mitchell 1998), and the methanol maser models require low gas temperatures so that the masers are not quenched by the deexciting collisions of the gas with the methanol molecules.

Walsh et al. (1998) agree with Norris et al. (1993) that there are more linear arrangements of methanol masers than can be explained by a chance probability in their survey. However, because most of the sites observed do not have a systematic velocity gradient, they feel that the circumstellar hypothesis could not explain all of the data. They suggest that an “expanding shock” model explains their data better. They contend that dense knots of material have been compressed and accelerated by the passage of a shock. These knots would not necessarily lie along the line of site to the UC H II region. If these knots of material lay far from the point of origin of the shock, it would explain why we often see methanol maser emission without a UC H II region present. They argue that since we observe the component of the shock velocity only along our line of sight, a shock wave impinging on several separated spots on the plane of the sky would show a smooth velocity gradient. In general, however, one would expect the shock wave to expand nonuniformly as it propagates through a inhomogeneous medium. Again, there is the problem of the postshock gas being high enough in temperature to quench the masers, unless some sort of efficient cooling mechanism is present.

Sobolev et al. (1997) find fault in the circumstellar disk hypothesis because the gas in the disk may be too hot. However, models show that disks are stratified, with a warm atmosphere above and below the disk, and a cooler dense central region. The warm material sandwiching the cooler disk could provide it with a large supply of mid-infrared photons for pumping. This seems consistent with our findings in § 5.3, which indicate that conditions for methanol maser emission lie within the mid-infrared emitting regions. The mid-plane of the disk would be cool enough to satisfy the low kinetic gas temperatures needed to avoid maser quenching. Also, the disk would have a density gradient, where densities lessen as one approaches the disk/disk-atmosphere interface. With the disk arranged so that the observer sees it nearly edge-on, the maser’s path would come through the disk at an angle which would contain the appropriate density needed for the existence of the maser. In this way, one may be able to explain the curved structures of the maser spots that lie in an arc. Furthermore, maser spot properties such as radial velocities, brightness, and location would be subject to many local variables in a disk where the turbulent velocities are compa-

rable to the disk's slow rotation. Therefore, one would not expect to always get velocity gradients along the spots, and a velocity gradient may not be a general property of methanol masers in disks. Thus, attempts to prove or disprove the circumstellar hypothesis on these grounds (i.e., deriving masses of central stars, and plotting position-velocity diagrams) may be futile.

Elitzur (1992) has suggested that OH masers can lie between the shock and ionization front of expanding UC H II regions. Interestingly, methanol masers are often spatially coincident with OH masers. This may indicate, contrary to the temperature argument about quenching, that the conditions in shock fronts may in fact be viable for the existence of methanol masers. Indeed, at least one source in our survey, G351.42+0.64:DPT00 1 (NGC 6334F), seems to have masers associated with the sharp western boundary of the extended UC H II region. Here the methanol masers exist spatially coincident with OH masers and seem to most likely to exist in the shock region of the UC H II region. There are also other sources in the survey that may be displaying methanol masers in an outflow. Water masers are known to exist in linear distributions that point radially away from UC H II regions, and so are thought to exist in shocks associated with outflow (Felli, Palagi, & Tofani 1992). In the same manner, we see sources in this survey where methanol masers are distributed radially with respect to the closest mid-infrared source, G323.741-0.263:DPT00 1 and G351.42+0.64:DPT00 3 (NGC 6334F-NW), for example. It therefore seems reasonable to assume that linearly distributed methanol masers, and methanol masers in general, can be associated with shocks, outflows, and disks.

## 6. CONCLUSIONS

We imaged 21 sites of known methanol maser emission at 10.46 and 18.06  $\mu\text{m}$ . Ten of the sites contained methanol masers distributed in a linear fashion. Of those 10 sites, there were eight detections, three of which have sources that are resolved and elongated in their thermal emission at the same position angle as the maser distribution. This data seems to lend credibility to the hypothesis of Norris et al. (1993) that linearly distributed methanol masers exist in and delineate circumstellar disks. However, linear methanol masers (and methanol masers in general) do not appear to be exclusively associated with circumstellar disks, but instead trace a variety of stellar processes. We find evidence that supports the idea that methanol masers are also associated with outflows and shocks as well.

The lower limits on the bolometric luminosity as derived from our mid-infrared flux densities imply that the stellar sources associated with methanol maser emission that do not have detectable UC H II regions are of smaller, less ionizing masses. The sources with earlier spectral types (as derived from the mid-infrared fluxes) between B1 and B6 contain detectable UC H II regions. The sources with spectral types between B7 and A4 do not have evidence of radio continuum. It has been argued by Walsh et al. (1998) and others, that the stellar sources without UC H II regions are at an earlier stage of evolution and are too deeply embedded and have not had time to ionize their surroundings. However, many of these sources are seen in the near-infrared as well as mid-infrared, and therefore cannot be too heavily embedded as to inhibit radio continuum emission. We conclude that the stellar sources associated with methanol maser emission that do not have any detectable radio continuum are stars of lower mass than those that do have detectable radio continuum.

There seems to be a rough correlation between maser distribution extent and the extent of the mid-infrared sources. We also find that the methanol masers are distributed in smaller areas than the mid-infrared emitting regions around these massive stars. If masers and mid-infrared emission peaks are assumed to be coincident, there is agreement with modeling by Sobolev & Deguchi (1994) and Sobolev et al. (1997) showing that the pumping is achieved via mid-infrared photons from dust with a temperature of more than 150 K.

We find that many of the sites of methanol maser emission have several mid-infrared sources in our  $23'' \times 23''$  field. Since this is much smaller than the *IRAS* imaging beam and LRS field of view, the flux density values and spectral features observed for these sites cannot be used to accurately describe or model the individual sources associated with the methanol masers.

We wish to thank the staff of the Cerro Tololo Inter-American Observatory for their outstanding observer's support and for their outstanding engineering support for visitor instrumentation. We also wish to thank Marie-Claire Hainaut for her invaluable help and multilingual skills, without which obtaining the observations presented in this paper would have been all the more difficult. This research was supported by the NASA Florida Space Grant Consortium grant NGT 5-40025 and the University of Florida.

## REFERENCES

- Andre, P., Ward-Thompson, D., & Barsony, M. 1993, *ApJ*, 406, 122  
 Bachiller, R., Codella, C., Colomer, F., Liechti, S., & Walmsley, C.M. 1998, *A&A*, 335, 266  
 Batrla, W., Matthews, H. E., Menten, K. M., & Walmsley, C.M. 1987, *Nature*, 326, 49  
 Bonnell, I. A. 1994, *MNRAS*, 269, 837  
 Carral, P., Kurtz, S. E., Rodriguez, L. F., De Pree, C., & Hofner, P. 1997, *ApJ*, 486, 103  
 Caswell, J. L. 1996, *MNRAS*, 279, 79  
 ———. 1997, *MNRAS*, 289, 203  
 Caswell, J. L., & Haynes, R. F. 1987, *A&A*, 171, 261  
 Caswell, J. L., Haynes, R. F., & Goss, W. M. 1980, *Australian J. Phys.*, 33, 639  
 Caswell, J. L., & Vaile, R. A. 1995, *MNRAS*, 273, 328  
 Caswell, J. L., Vaile, R. A., Ellingsen, S. P., Whiteoak, J. B., & Norris, R. P. 1995, *MNRAS*, 272, 96  
 Caswell, J. L., Vaile, R. A., & Forster, J. R. 1995, *MNRAS*, 277, 210  
 Cesaroni, R., Churchwell, E., Hofner, P., Walmsley, C. M., & Kurtz, S. 1994, *A&A*, 288, 903  
 Chan, S. J., Henning, T., & Schreyer, K. 1996, *A&AS*, 115, 285  
 Churchwell, E. 1991, in *The Physics of Star Formation & Early Stellar Evolution*, ed. C. J. Lada & N. D. Kylafis (Dordrecht: Kluwer), 221  
 Doyon, R. 1990, Ph.D. thesis, Imperial College, Univ. London  
 Elitzur, M. 1992, *ARA&A*, 30, 75  
 Ellingsen, S. P., Norris, R. P., & McCulloch, P. M. 1996, *MNRAS*, 279, 101  
 Felli, M., Palagi, F., & Tofani, G. 1992, *A&A*, 255, 293  
 Fix, J. D., Mutel, R. L., Gaume, R. A., & Claussen, M. J. 1982, *ApJ*, 259, 657  
 Forster, J. R. 1990, *A&A*, 227, L37  
 Forster, J. R., & Caswell, J. L. 1989, *A&A*, 213, 339  
 Forster, J. R., Caswell, J. L., Okumura, S. K., Ishiguro, M., & Hasegawa, T. 1990, *A&A*, 231, 473  
 Frail, D. A., & Mitchell, G. F. 1998, *ApJ*, 508, 690  
 Garay, G., Rodriguez, L. F., Moran, J. M., & Churchwell, E. 1993, *ApJ*, 418, 368  
 Gaume, R. A., & Mutel, R. L. 1987, *ApJS*, 65, 193  
 Goebel, J. H. 1993, *A&A*, 278, 226  
 Harvey, P. M., & Gatley, I. 1983, *ApJ*, 269, 613  
 Haynes, R. F., Caswell, J. L., & Simons, L. W. J. 1979, *Australian J. Phys. Astrophys. Suppl.*, 48, 1

- Henning, T., Chan, S. J., & Assendorp, R. 1996, *A&A*, 312, 511
- Hofner, P., & Churchwell, E. 1996, *A&AS*, 120, 283
- Hofner, P., Kurtz, S., Churchwell, E., Walmsley, C. M., & Cesaroni, R. 1994, *ApJ*, 429, 85
- Hrivnak, B. J., Kwok, S., & Geballe, T. R. 1994, *ApJ*, 420, 783
- Hughes, V. A., & MacLeod, G. C. 1993, *AJ*, 105, 1495
- IRAS* Science Team 1986, *A&AS*, 65, 607
- Jensen, E. L. N., Donar, A. X., & Mathieu, R. D. 2000, in *Birth and Evolution of Binary Stars*, ed. B. R. Reipurth & H. Zinnecker (Potsdam: IAU), 85
- Kraemer, K. E., Deutsch, L. K., Jackson, J. M., Hora, J. L., Fazio, G. G., Hoffmann, W. F., & Dayal, A. 1999, *ApJ*, 516, 817
- Kemball, A. J., Gaylard, M. L., & Nicolson, G. D. 1988, *ApJ*, 331, 37
- Kurtz, S., Churchwell, E., & Wood, D. O. S. 1994, *ApJS*, 91, 659
- Kurucz, R. L. 1979, *ApJS*, 40, 1
- Lada, C. J. 1987, in *Star-Forming Regions*, ed. M. Peimbert & J. Jugaku (Dordrecht: Reidel), 1
- MacLeod, G. C., Gaylard, M. J., & Nicolson, G. D. 1992, *MNRAS*, 254, 1P
- MacLeod, G. C., Scalise, E., Saedt, S., Galt, J. A., & Gaylard, M. J. 1998, *AJ*, 116, 1897
- Mathis, J. S. 1990, *ARA&A*, 28, 37
- Menten, K. M. 1991a, in *Proc. Third Haystack Observatory Meeting, Skylines*, ed. A. D. Haschick & P. T. P. Ho (San Francisco: ASP), 119
- . 1991b, *ApJ*, 380, 75
- Monin, J.-L., Menard, F., & Duchene, G. 1998, *A&A*, 339, 113
- Neckel, T. 1978, *A&A*, 69, 51
- Norris, R. P., Caswell, J. L., Gardner, F. F., & Wellington, K. J. 1987, *ApJ*, 321, 159
- Norris, R. P., et al. 1998, *ApJ*, 508, 275
- Norris, R. P., Caswell, J. L., Wellington, K. J., McCutcheon, W. H., & Reynolds, J. E. 1988, *Nature*, 335, 149
- Norris, R. P., Whiteoak, J. B., Caswell, J. L., Wieringa, M. H., & Gough, R. G. 1993, *ApJ*, 412, 222
- Omont, A., et al. 1995, *ApJ*, 454, 819
- Osterloh, M., Henning, Th., & Launhardt, R. 1997, *ApJS*, 110, 71
- Panagia, N. 1973, *AJ*, 78, 929
- Phillips, C. J., Norris, R. P., Ellingsen, S. P., & McCulloch, P. M. 1998, *MNRAS*, 300, 1131
- Rodriguez, L. F., Canto, J., & Moran, J. M. 1982, *ApJ*, 255, 103
- Sobolev, A. M., & Deguchi, S. 1994, *A&A*, 291, 569
- Sobolev, A. M., Cragg, D. M., & Godfrey, P. D. 1997, *A&A*, 324, 211
- Stecklum, B., & Kauf, H. 1998, *First Circumstellar Disk around a Massive Star* (ESO press release PR-08-98)
- Tofani, G., Felli, M., Taylor, G. B., & Hunter, T. R. 1995, *A&AS*, 112, 299
- van der Walt, D. J., Gaylard, M. J., & MacLeod, G. C. 1995, *A&AS*, 110, 81
- Volk, K., Kwok, S., Stencel, R. E., & Brugel, E. 1991, *ApJS*, 77, 607
- Walsh, A. J., Burton, M. G., Hyland, A. R., & Robinson, G. 1998, *MNRAS*, 301, 640
- Walsh, A. J., Burton, M. G., Hyland, A. R., & Robinson, G. 1999, *MNRAS*, 309, 905
- Walsh, A. J., Hyland, A. R., Robinson, G., & Burton, M. G. 1997, *MNRAS*, 291, 261
- Wink, J. E., Altenhoff, W. J., & Mezger, P. G. 1982, *A&A*, 108, 227
- Zinchenko, I., Mattila, K., & Toriseva, M. 1995, *A&AS*, 111, 95